buildings

MDPI

Review

Behavior of Fibers in Geopolymer Concrete: A Comprehensive Review

Ujjwal Sharma [1], Nakul Gupta [2], Alireza Bahrami [3,*], Yasin Onuralp Özkılıç [4,5,*], Manvendra Verma [2], Parveen Berwal [6], Essam Althaqafi [7], Mohammad Amir Khan [6] and Saiful Islam [7]

[1] Department of Civil Engineering, Ixrlabs Learning Solutions Pvt. Ltd., Jaipur 302021, India
[2] Department of Civil Engineering, GLA University, Mathura 281406, India
[3] Department of Building Engineering, Energy Systems and Sustainability Science, Faculty of Engineering and Sustainable Development, University of Gävle, 801 76 Gävle, Sweden
[4] Department of Civil Engineering, Faculty of Engineering, Necmettin Erbakan University, Konya 42000, Turkey
[5] Department of Civil Engineering, Lebanese American University, Byblos 1102-2801, Lebanon
[6] Department of Civil Engineering, Galgotias College of Engineering and Technology, Greater Noida 201310, India
[7] Civil Engineering Department, College of Engineering, King Khalid University, Abha 61421, Saudi Arabia
* Correspondence: alireza.bahrami@hig.se (A.B.); yozkilic@erbakan.edu.tr (Y.O.Ö.)

Abstract: Over the last decades, cement has been observed to be the most adaptive material for global development in the construction industry. The use of ordinary concrete primarily requires the addition of cement. According to the record, there has been an increase in the direct carbon footprint during cement production. The International Energy Agency, IEA, is working toward net zero emissions by 2050. To achieve this target, there should be a decline in the clinker-to-cement ratio. Also, the deployment of innovative technologies is required in the production of cement. The use of alternative binding materials can be an easy solution. There are several options for a substitute to cement as a binding agent, which are available commercially. Non-crystalline alkali-aluminosilicate geopolymers have gained the attention of researchers over time. Geopolymer concrete uses byproduct waste to reduce direct carbon dioxide emissions during production. Despite being this advantageous, its utilization is still limited as it shows the quasi-brittle behavior. Using different fibers has been started to overcome this weakness. This article emphasizes and reviews various mechanical properties of fiber-reinforced geopolymer concrete, focusing on its development and implementation in a wide range of applications. This study concludes that the use of fiber-reinforced geopolymer concrete should be commercialized after the establishment of proper standards for manufacturing.

Keywords: geopolymer concrete; fiber-reinforced concrete; mechanical behavior; microstructural analysis; compressive strength; flexural strength

check for updates

Citation: Sharma, U.; Gupta, N.; Bahrami, A.; Özkılıç, Y.O.; Verma, M.; Berwal, P.; Althaqafi, E.; Khan, M.A.; Islam, S. Behavior of Fibers in Geopolymer Concrete: A Comprehensive Review. *Buildings* **2024**, *14*, 136. https://doi.org/10.3390/buildings14010136

Academic Editor: Ciro Del Vecchio

Received: 9 September 2023
Revised: 8 November 2023
Accepted: 28 November 2023
Published: 4 January 2024

1. Introduction

In recent decades, there has been a rapid growth in urbanization in both less and more developed countries [1]. By 2050, approximately more than two-thirds of the world's population is expected to move to urban areas [2]. Globally, in 2018, the share of the urban population was around 4.2 billion, whereas 3.4 billion people were reported to live in rural areas. But by 2050, the statistics will change and around 6.7 billion people will live in urban areas and only 3.1 billion people will live in rural areas [2]. Urbanization along with the emerging population growth is the major cause of the increasing demand for concrete [3–6]. Concrete existence is mainly due to the cohesive strength of cement, which increases rapidly during setting [7]. Globally, no sign of decline was observed in the production of Portland cement (PC), indicating that it has been increasing continuously [8–10]. A large number of natural resources are used for the production of PC like fossil fuels, limestone, electricity, and natural gas [8]. The manufacturing of PC is a very high-temperature and energy-intensive process, which results in an increase in carbon dioxide (CO_2) footprint in the atmosphere [11–22]. The carbon emissions are primary factors contributing to global warming. Between 2015 and 2020, the direct CO_2 intensity of cement manufacturing grew by 1.8 percent per year. An annual reduction of 3% is required by 2030 to meet the final requirement of net zero emissions by 2050 [23]. Cement is made up primarily of clinker, which is directly proportional to CO_2 emitted due to limestone decomposition in the clinker-making process and from fuel combustion [13,23–27]. Therefore, to reduce the effect of carbon footprint due to PC production, particularly process emission, there is a need for alternative (sustainable) binding materials [18,23,27–31].

The rise in the use of concrete across various applications resulted in an increase in concrete consumption [32–36]. This also led to the development of concrete in different perspectives [37–41], which resulted in the invention of geopolymer concrete. For decades, researchers have been showing interest in geopolymer, an inorganic polymer with low density and high-temperature tolerance [42–46]. It is a sustainable and environmentally friendly substitute to PC with a low cost of production [42–44,47–49]. Geopolymer concrete technology offers significant promise for the commercialization, standardization, and repurposing of agricultural and industrial byproducts [50–53]. Research has been carried out to address the challenges of environmental contamination caused by the disposal of these wastes in landfills [50]. Depending on the use of activators and precursors, an 80% reduction in the footprint of carbon has been observed while using geopolymer [54–57]. Moreover, a comprehensive survey has been conducted and the results demonstrated that alkali-activated binding materials have high strength, low carbon content, good frost resistance, etc. [58,59]. Researchers acknowledged the use of geopolymer in retaining walls, boundary blocks, pavements, water tanks, road ramps, and precast beams. Despite all the applications of geopolymer, its application is still considerably limited. This is owing to limited studies on its use in structural elements and due to the requirements of practical design standards [60].

Various studies on geopolymer have identified that it displays quasi-brittle behavior like PC concrete and rocks [61–65]. Structures that exhibit large macroscopic crack growth prior to failure are termed quasi-brittle structures [66,67]. To overcome this failure, the use of distinct fibers, whether continuous or short fibers along with alkali-activated binders, is introduced [67–69]. This article offers a comprehensive and pioneering exploration of the mechanical properties of fiber-reinforced geopolymer concrete (FRGC), emphasizing its development and practical application. While some research works may overlook the importance of incorporating various fibers alongside alkali-activated binders to bolster the structural strength of geopolymer concrete, our study underscores this critical factor. Our examination of the material's mechanical behavior provides valuable insights which are crucial for real-world applications, setting our work apart from studies that primarily focus on binders. Additionally, our research goes a step further by categorizing different types of fibers based on characteristics such as type, aspect ratio, strength, modulus of elasticity, and density. This classification facilitates the prioritization of specific fiber types according to their impact on the mechanical properties, a novel contribution that was previously absent in the existing body of literature on FRGC.

In this study, the research on geopolymer concrete holds remarkable importance for sustainable construction practices. Geopolymer, characterized by low density and high-temperature tolerance, emerges as an eco-friendly alternative to traditional PC, contributing to reduced carbon footprints and waste management. It effectively utilizes agricultural and industrial residues, mitigating environmental contamination from landfill disposal. However, despite its potential, the adoption of geopolymer concrete remains limited, primarily due to the absence of practical design standards for structural elements. This research addresses a critical issue by focusing on FRGC, a vital aspect often overlooked in prior studies. By incorporating various fibers alongside alkali-activated binders, the study enhances the structural strength of geopolymer concrete. Moreover, it classifies fibers based on their characteristics, allowing for the prioritization of specific fiber types in accordance with their influence on the mechanical properties. This novel contribution fills a significant gap in the existing literature and provides valuable insights for real-world applications. This research work extends the potential of geopolymer concrete by improving its structural integrity and providing a comprehensive framework for incorporating different fiber types, making it a crucial step toward wider adoption of this sustainable construction material.

The existing research gap in fiber-reinforced geopolymer composites lies in the insufficient attention to the economic feasibility and scalability of these materials. While extensive studies have focused on their technical properties, there is a need for investigation into the cost effectiveness of large-scale production and implementation in construction projects. Additionally, the environmental impact of fiber-reinforced geopolymer composites, including factors such as raw material sourcing and energy consumption during production, requires further scrutiny. Bridging this research gap will be pivotal in ensuring that geopolymer composites not only exhibit impressive technical performance, but also prove to be economically viable and environmentally sustainable for widespread adoption in the construction industry.

2. Geopolymer

In the 1970s, a supplement to cement with ceramic-like properties termed as geopolymer was introduced by Davidovits [70–72]. The process to produce geopolymers involves the co-polymerization of alumina and silica components [73]. Geopolymer can harden to form a binder due to polymerization and transformation [74]. Geopolymer materials have a chemical composition like natural zeolitic materials, but their microstructure is amorphous rather than crystalline [75–78]. Its basic framework structure comprises silicon–oxygen–aluminum; therefore, it is an inorganic polymer [71,74,79,80]. Furthermore, geopolymer possesses 3D silico-aluminate structures of varying silica to alumina ratio, which are designated as poly-sialate, poly-sialate-siloxo, and poly-sialate-disiloxo with (Si:Al = 1), (Si:Al = 2), and (Si:Al > 3), respectively [75,81–83]. Geopolymerization involves the chemical reaction of naturally occurring alumino silicates [57,84]. In addition, geopolymer has two parts: one is a precursor (any pozzolanic material which includes part of alumina and silica and is readily dissolved in alkaline solution) and the other one is an activator (alkali component) [57,85,86]. Various researchers have proposed different reaction phases to explain manufacturing of geopolymer [48,87,88]:

Dissolution: The precursors (alumino-silicate minerals) [85,89] dissolved with activators (alkali component with pH > 7) [85].

Re-orientation: Monomers of liberated silicate and aluminate combine to form short alumino-silicate oligomers.

Solidification: The 3D geopolymer structure hardens and gains strength.

Completion of these three reaction phases is related to the characteristics of various alumino-silicate source materials. Proper dissolution is accomplished by sodium silicate (Na_2SiO_3 with pH range of 11–13) and sodium hydroxide (NaOH with pH of 14) solutions [90–92]. The introduction of a resting period between mixing and shaping the material and the commencement of solidification by adding heat are common ways to stimulate the reorientation phase [83]. The compressive strength development after geopolymer hardening starts at room temperature for various pozzolanic materials. N-A-S-H gel is a 3D structure, which is found to be the main hydration product of this calcium-free binder [93]. The alkaline solution has an impact on both fresh and hardened properties of geopolymer concrete; therefore, the selection should be made carefully [55]. Both precursors (alumino-silicate materials) and activators (alkaline solutions) are dependent on the strength development of geopolymeric materials [94].

The objective of this review article on geopolymer concrete is as follows:

a. To develop a better understanding of alumino-silicate material.
b. To study the temperature effect and curing time.
c. To gather the knowledge regarding the selection or use of the proper alkaline activator solution.

d. To study the proper water content.

3. FRGC

When various types of fibers such as composite fillers are added to geopolymer, their composition is considered an FRGC [95–98]. These FRGC composites enhance the structural durability as they can sustain temperatures from as low as room temperature to higher elevated temperatures (for example, 1000 °C) [34,86–88]. Consequently, these FRGC composites are an emerging alternative to repair materials in the construction industry [99–101]. The processing ability of these composites can be affected by the fiber length. As a result, they are classified as short fiber composites (length of less than 1 mm) and long fiber composites (length of more than 2 mm and up to 10 mm) [102]. The use of the geopolymer matrix with fibers is found to be admissible as they can sustain elevated temperatures with excellent durability and no release of toxic gas [96,103–105]. Therefore, to improve the energy absorption and modulus of rupture (flexural strength), geopolymer composites are reinforced with fibers in various forms of filaments, threads, whiskers, and nanoparticles [106]. The selection of fibers to make FRGC composites is based on a sufficient fiber–matrix interaction, material property compatibility with applications, and optimum aspect ratio to control the post-cracking behavior of these composites [106]. Accordingly, fibers are classified as metallic fibers (such as steel fiber), mineral fibers (such as asbestos fiber), organic fibers (natural and man-made fiber), natural fibers (such as leaf fiber and silk), natural polymers (such as protein fiber and cellulose), and synthetic fibers (such as polypropylene and nylon fibers) based on the origin of the fibers [107]. In regard to the fibers, researchers have proposed that the performance of FRGC composites predominantly depends on the properties of the fibers [106].

4. Effect of Fibers on FRGC

4.1. Steel Fiber

Steel fibers can be defined as a metal reinforcement with a discrete length and aspect ratio in a range between 20 and 100, in which various cross sections can be randomly dispersed in fresh concrete mixture [108]. Steel fiber-reinforced concrete (SFRC) has a wide range of applications in civil engineering [109] such as enhancing the toughness, impact, and abrasion resistance of various composites [108]. Owing to the high availability, mechanical strength, and flexibility of steel fibers, they are used in cement composites [106]. Modified cold-drawn wires, mill cut, melt extracted, pieces of smooth or deformed cold-drawn wires and smooth or deformed cut sheet steel fibers are categorized as types of steel fibers according to ASTM A820-16 [110]. The fibers are categorized based on their physical and mechanical properties. From the literature, it is acknowledged that for different types of steel fibers with a distinct aspect ratio, the modulus of elasticity was approximately 2×10^5 MPa, and the fiber strength ranges between 800 and 2850 (MPa) with an approximate density of 7.8 kg/m^3. Table 1 lists the physical and mechanical properties of steel fibers. The microstructural properties (sorptivity, effective porosity, and water absorption) of geopolymer concrete were lower than conventional concrete, which can be further improved with the addition of a lower quantity of steel fibers. Furthermore, it can be concluded that the durability characteristics of geopolymer concrete is better than conventional concrete, which can be further improved with the addition of steel fibers [111]. For the ultra-high-performance fiber-reinforced geopolymer concrete (UHPFRGC), 2% (by volume fraction) of steel fibers gives the highest mechanical strength. Whereas the mechanical strength of UHPFRGC reduces when steel fibers are replaced with polypropylene fibers. For concrete with both steel fibers and polypropylene fibers, the flow passing through concrete is reduced [112]. Riahi et al. [113] concluded in their research that the interfacial bond between the metakaolin-based polymer composite and steel fibers affects the strength. Figure 1 depicts a scanning electron microscope (SEM) image of an uncoated steel fiber matrix transition zone, revealing the debonding that occurs at the interface. In Figure 2, another SEM image illustrates the same uncoated steel fiber matrix transition zone, but this time, it highlights the presence of a geopolymeric product adhering to the surface of steel fibers. Figure 3 presents a SEM image indicating the interface between a steel-coated fiber matrix and the alumina coating in the transition zone. Meanwhile, Figure 4 showcases another SEM image demonstrating the debonding process and the presence of geopolymer products on the surface of coating. Thus, to increase the interfacial bond strength between the polymer composite and steel fibers, an alumina coating should be done on steel fibers. Compared to the uncoated steel fibers, the alumina-coated steel fibers enhanced the bond strength by 151%. It was also resulted from the study that the peak load deflection and deflection hardening behavior of the alumina-coated steel fibers were higher.

Table 1. Details of different types of steel fibers.

Fiber Type	Aspect Ratio	Modulus of Elasticity (MPa)	Strength (MPa)	Density (g/cm^3)	Reference
Steel fiber	83.3	200,000	2500	7.8	[114]
Steel fiber	65	200,000	2000	7.850	[112]
Micro steel fiber	30	NA	>2600	7.9	[115]
Micro steel fiber	91.66	210,000	-	7.8	[115]
Deformed macro steel fiber	32.72	NA	800	7.865	[115]
Straight steel fiber (SS)	50	-	2500	7.850	[116]
Straight steel fiber (SM)	67	-	2500	7.850	[116]
Straight steel fiber (SW)	65	-	2850	7.850	[116]
Hooked-end steel fiber	65	-	2850	7.850	[116]
Hooked-end steel fiber	81.33	210,000	1350	7.850	[117]
Straight steel fiber (SL)	108	-	2500	7.850	[118]
Hooked-end steel fiber	64	-	1345	7.850	[119]
Hooked-end steel fiber	45	-	1225	7.850	[113]
Hooked-end steel fiber	65	210,000	1350	-	[120]
Hooked-end steel fiber	54.55	200,000	1500	7.850	[121]
Hooked-end steel fiber	83.33	200,000	2500	7.80	[122]
Spiral steel fiber	45.45	200,000	1400	7.80	[122]

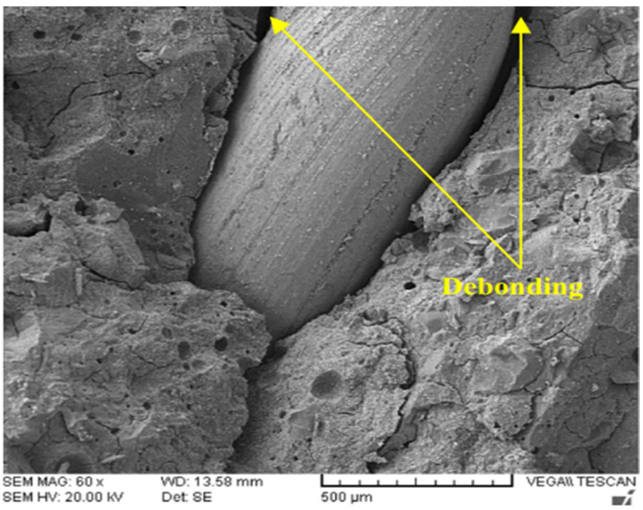

Figure 1. SEM image of uncoated steel fiber matrix transition zone showing debonding process at interface. Reprinted/adapted with permission from Ref. [113], 2021, Elsevier Ltd. All rights reserved.

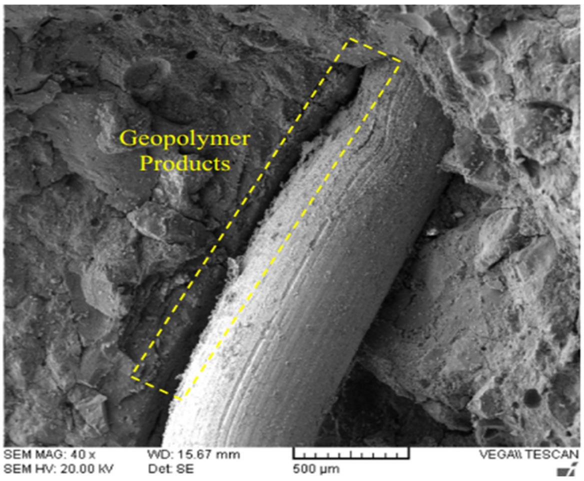

Figure 2. SEM image of uncoated steel fiber matrix transition zone showing geopolymeric product on surface of steel fibers. Reprinted/adapted with permission from Ref. [113], 2021, Elsevier Ltd.

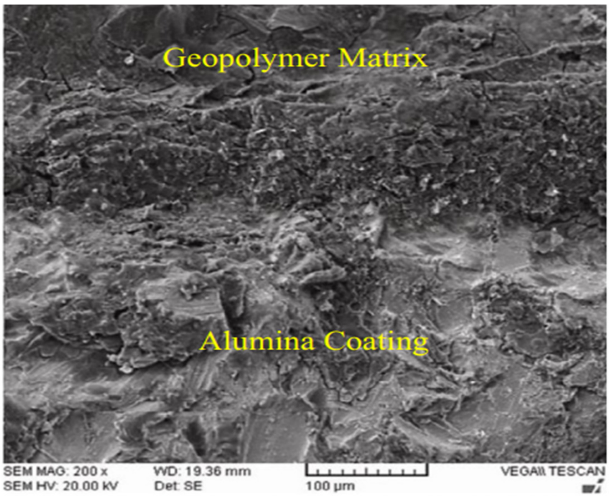

Figure 3. SEM image of alumina-coated steel fiber matrix transition zone showing steel-coated fiber matrix interface. Reprinted/adapted with permission from Ref. [113], 2021, Elsevier Ltd.

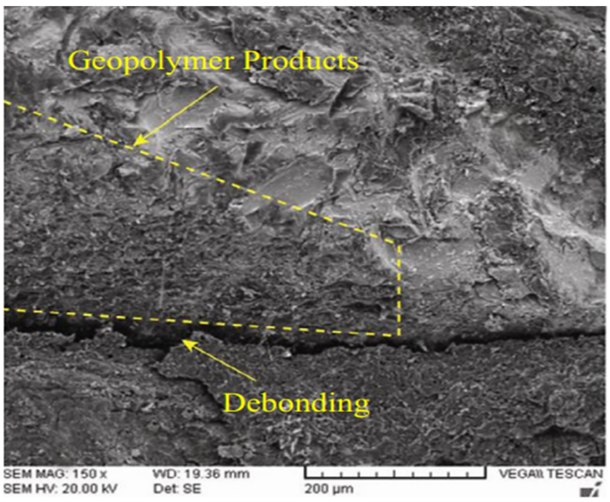

Figure 4. SEM image showing debonding process and geopolymeric products on coating surface. Reprinted/adapted with permission from Ref. [113], 2021, Elsevier Ltd.

Figure 5 displays the coil diameter, nominal length, and pitch length of a spiral steel fiber. Figure 6 illustrates what a steel fiber with hooked ends looks like.

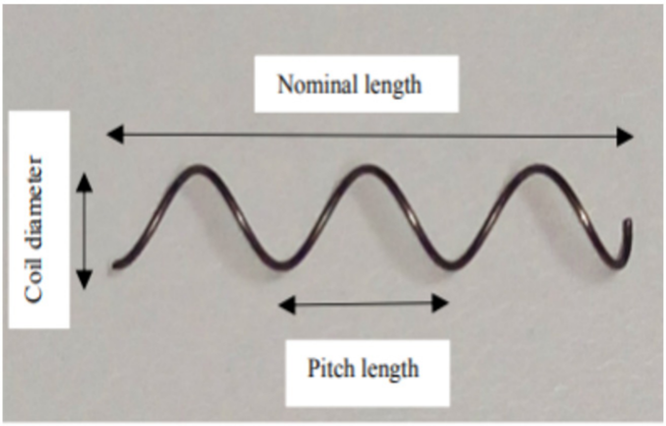

Figure 5. Spiral steel fiber. Reprinted/adapted with permission from Ref. [122], 2019, Elsevier Ltd.

Figure 6. Steel fibers with hooked ends. Reprinted/adapted with permission from Ref. [121], 2018, Elsevier Ltd.

According to [123], the elevated temperature also affects the compressive strength of steel fiber-reinforced geopolymer concrete (SFRGC) for both sodium and potassium alkali-activator based concretes. The strength up to a temperature of 400 °C was higher compared to concrete cured in ambient temperature and to that of SFRC. However, it tends to decrease in the same pattern for all types of concrete. Alkali-activated based geopolymer concretes (concrete with sodium hydroxide and concrete with potassium hydroxide) at elevated temperatures exhibit a lower elastic modulus compared to that of SFRC. Taking SFRC into consideration, both alkali-activator concretes experience lesser spalling at an ultimate compression load and lesser surface cracking when exposed to elevated temperatures. Also, the damage in the top layer of steel fibers is noticed in the case of SFRC compared to both SFRGC (with sodium hydroxide) and SFRGC (with potassium hydroxide) when exposed to elevated temperatures.

Liu et al. [116] evaluated the influence of steel fibers on the mechanical properties of ground granulated blast-furnace slag (GGBS), silica fume, and class F fly ash-based geopolymer concrete. They compared the effect of straight steel fibers on the compressive and flexural strengths of SFRGC with three different aspect ratios at three various volume fractions. Table 1 provides the details of the fibers used in the research. Three different fiber types are named as SM (straight steel fiber with an aspect ratio of 67 and tensile strength of 2500 MPa), SL (straight steel fiber with an aspect ratio of 108 and tensile strength of

2500 MPa), and SW (straight steel fiber with an aspect ratio of 65 and tensile strength of 2850 MPa). The three volume fractions were 1%, 2%, and 3%. Figures 7 and 8 depict a comparison of 28-day compressive strength and 28-day flexural strength, respectively for various SM, SL, and SW specimens of SFRGC. In Figures 7 and 8, SM1, SM2, and SM3 designate specimens with 1%, 2%, and 3% SM type of steel fibers, respectively. SL1, SL2, and SL3 represent specimens with 1%, 2%, and 3% SL type of steel fibers, respectively. SW1, SW2, and SW3 denote specimens with 1%, 2%, and 3% SW type of steel fibers, respectively. The figures point out that for all three different types of fiber specimens (SM, SL, and SW), both the compressive strength and flexural strength increased with an increase in the percentage of fibers from 1% to 3%. Among all the considered specimens, SL3 gave the best result for both compressive strength and flexural strength with values of 170.4 MPa and 33.3 MPa, respectively. The comparison concludes that fibers with a higher aspect ratio would perform well [116]. Table 2 consists of the literature survey on SFRGC.

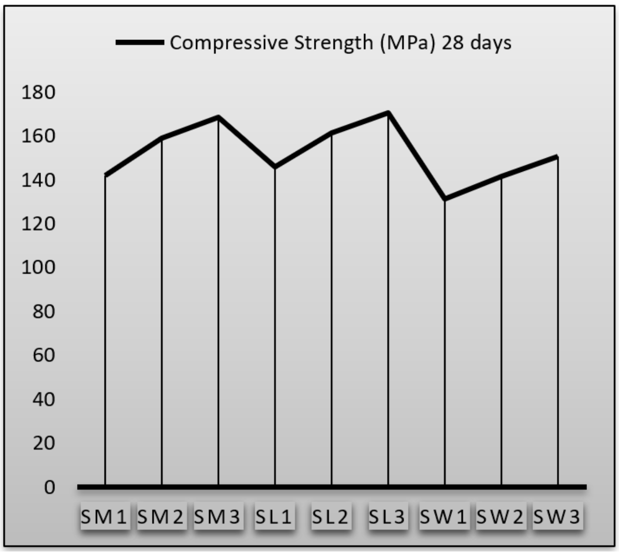

Figure 7. Effect of straight steel fibers with different aspect ratios on compressive strength of SFRGC [116].

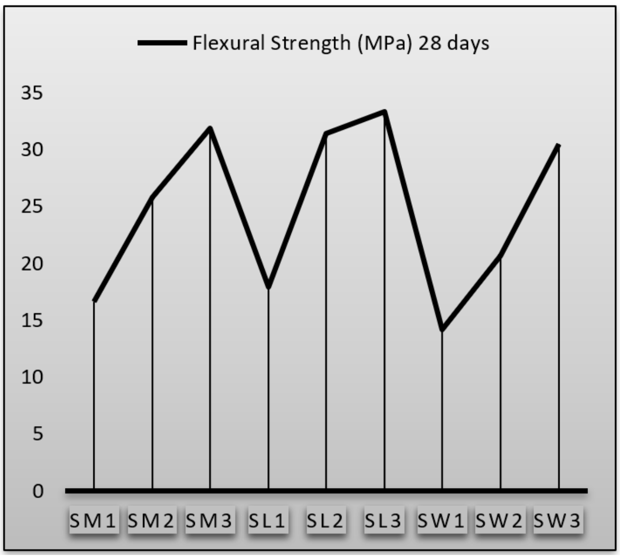

Figure 8. Effect of straight steel fibers with different aspect ratios on flexural strength of SFRGC [116].

Table 2. Literature survey on SFRGC.

Reference	Precursor Type	Activator Type	Molarity	Fiber Content	Aspect Ratio	Curing Type	Effect
[111]	Fly ash (Class C)	NaOH + Na_2SiO_3	10 M	(by volume fraction)	60	Heat curing	Enhanced compressive, flexural, and splitting tensile strength at 28 days. Reduced slump and compaction factor. Higher abrasion resistance compared to cement concrete. Excellent resistance to acid and sulphate attack.
[124]	Fly ash GGBS Kaolite (HPA)	NaOH + Na_2SiO_3	12 M	(by volume fraction)	63.63 and 65	Ambient curing	Increase in fiber volume tends to increase the ultimate strength and cracking load. In composites with the low fiber content, propagation of cracks seems to be at a faster rate. Finer cracks were observed in beams with higher fiber content.
[123]	Fly ash (Class F)	NaOH + Na_2SiO_3 and KOH + K_2SiO_3	8 M (NaOH) and 8 M (KOH)	0.5% and 0.75% Hooked-end fiber (by volume fraction)	66.6	Heat curing	Exhibit lower modulus of elasticity at elevated temperatures (similarly for both SFRGC (with sodium hydroxide) and SFRGC (with potassium hydroxide)). Increase in the compressive strength for both SFRGCs containing sodium and potassium activators (similarly in both ambient and elevated temperatures).
[125]	GGBS	NaOH + Na_2SiO_3	13 M	NA	NA	Ambient curing	Increase in the fiber content improves the impact strength. Increase in the compressive and splitting tensile strengths. Increase in the flexural strength of SFRGC.
[126]	Fly ash (Class F) + GGBS	NaOH + Na_2SiO_3	8 M 10 M 14 M	0.5%, 1.0%, 1.5%, 2.0%, and 3.0% Hooked-end fiber (by volume fraction)	65	Ambient curing	Increase in the fiber content enhances the compressive strength and flexural strength up to the optimum replacement value of 3%. There is a positive effect on the molarity of sodium hydroxide in the compressive strength increment.

Table 2. *Cont.*

Reference	Precursor Type	Activator Type	Molarity	Fiber Content	Aspect Ratio	Curing Type	Effect
[127]	Palm oil fuel ash + GGBS	NaOH + Na_2SiO_3	12 M	0.5% Hooked-end fiber (by volume fraction)	65	Ambient curing	Increased aggregate (oil palm shell) content tends to decrease the density and mechanical strength of concrete. The use of normal weight aggregate improves the mechanical properties of FRGC. All the fiber-reinforced oil palm shell geopolymer concrete specimens resisted high-impact loads before failure and produced smaller crack widths compared to oil palm shell geopolymer concrete.
[128]	Fly ash	NaOH + Na_2SiO_3	14 M	0%, 0.25%, 0.50%, 0.75%, and 1.0% Crimped steel fiber (by volume fraction)	66	Steam curing	Steel fiber addition enhances the cracking characteristics and tension stiffening of geopolymer concrete. 1% by volume fraction improves the first crack load. The prediction of cracks in geopolymer concrete by CEB-FIP (1990) proved to be more accurate than by Eurocode 2 (CEN, 2004).
[129]	Fly ash (Class F)	NaOH + Na_2SiO_3	-	0%, 0.5%, 1.0%, and 1.5% (by volume fraction)	60 70	Heat curing	Enhanced mechanical properties of SFRGC, especially the flexural strength. 1.0% is the optimum fiber content.
[130]	GGBS + Dolomite	NaOH + Na_2SiO_3	12 M	0%, 0.25%, 0.5%, 0.75%, and 1.0% Crimped steel fiber (by volume fraction)	60	Ambient curing	SFRGC with GGBS and dolomite increases the resistance of composite toward sulphate, chloride, acid, and saline water attack.

4.2. Glass Fiber

Glass fibers are non-crystalline materials with a short-range network structure that comprises an extremely fine fiber of glass [131]. Primarily, glass fibers are used to reinforce polymers. Generally, there are three leading glass fiber types including CR (corrosion resistant) glass, E-glass, and HS (high strength) glass [132]. When comparing E-glass and HS glass, HS glass has better creep and fatigue resistances. Glass fibers have low electrical as well as thermal conductivity. Kumar et al. [133] concluded that geopolymer concrete (combination of GGBS, fly ash, condensed silica fume, and metakaolin) with steel fibers increases the strength compared to concrete incorporated with glass fibers. But if the strength is not a major criterion, then glass fibers in geopolymer concrete play an important role. They make concrete denser, ductile, and crack free. Sivaraja et al. [134] reported that the compressive strength of geopolymer concrete with glass fibers, when heat cured at 60 °C, was found to be highest at 2% glass fibers by the volume fraction, and the splitting tensile strength was resulted to be highest at 2% fiber incorporation. The use of nano $CaCO_3$ in geopolymer acts as a nucleation site, which helps in the formation of additional products within the geopolymeric composite and in accelerating the geopolymeric reaction [135]. The ability of nanomaterials to fill micro voids helps the geopolymeric composite gain the strength. As a consequence, the research concluded that the incorporation of nano $CaCO_3$ increased the compressive strength, and the incorporated glass fibers improved the mechanical performance [135]. In accordance with Sathanandam et al. [136], the molarity of geopolymer concrete also affects the mechanical performance. The geopolymeric paste with molarity of 16 M and 20 M showed higher compressive strength than geopolymer concrete with 12 M. Additionally, 0.3% glass fibers incorporated with 20 M in geopolymer concrete, when cured thermally, demonstrated higher compressive strength than geopolymer concrete cured in a normal environment. Moreover, the addition of glass fibers to geopolymer concrete influenced the workability; the slump value decreased with the increase in the fiber content up to 1.25% by volume of concrete and the density increased with the increase in the fiber content by volume [137]. Geopolymer concrete without glass fibers exhibited both initial and final cracks at the same number of blows. But with glass fibers, the impact of geopolymer composite's strength increased ten times when compared to the control specimens, since fibers increased the modulus of elasticity and stiffness [138]. Figure 9 displays a SEM image of geopolymer concrete lacking the glass fiber reinforcement. This image visually elucidates the microstructure and composition of unreinforced concrete. In Figure 10, a SEM image of geopolymer concrete can be observed which has been fortified with 0.3% glass fibers, enabling us to scrutinize alterations in the structure and the distribution of fibers within the geopolymer matrix.

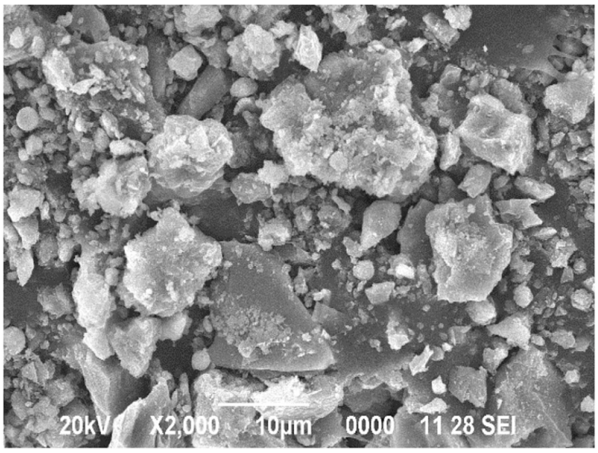

Figure 9. SEM image of geopolymer concrete with 0% glass fiber. Reprinted/adapted with permission from Ref. [136], 2017, Chinese Institute of Environmental Engineering, Taiwan. Production and hosting by Elsevier B.V.

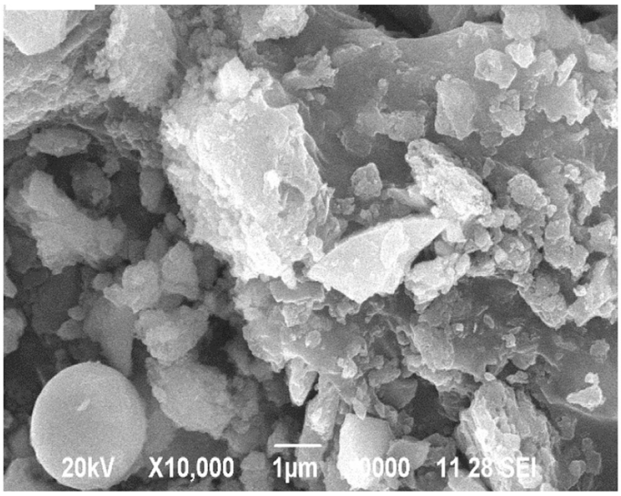

Figure 10. SEM image of glass fiber-reinforced geopolymer concrete (GFRGC) with 0.3% glass fibers. Reprinted/adapted with permission from Ref. [136], 2017, Chinese Institute of Environmental Engineering, Taiwan. Production and hosting by Elsevier B.V.

The addition of glass fibers to geopolymer concrete has illustrated varying effects on the compressive strength [136,139]. According to Table 3 of this research article, glass fibers are classified on the basis of their aspect ratio, length, diameter, modulus of elasticity, and tensile strength. Glass fibers used in the experimental investigations of Refs. [136,139] had aspect ratios of 35, 62, and 600, modulus of elasticity of 42,000 MPa and 82,000 MPa, respectively, and fibers' tensile strength of 1000 MPa and 2500 MPa, respectively. Zuaiter et al. [139] indicated that the incorporation of glass fibers led to the enhanced compressive strength at different curing ages. The short glass fibers resulted in an increase in the strength up to 24%, while the long fibers initially decreased the strength at 7 days but later increased at 28 days. Hybrid combinations, particularly with more long fibers at 1% volume fraction, showed a substantial 40% increase in the strength. On the other hand, Sathanandam et al. [136] highlighted that the inclusion of 0.3% glass fibers in geopolymer concrete resulted in a notable 16% increase in the compressive strength compared to the conventional geopolymer concrete. However, the addition of fibers led to the reduced strength. From the above comparison, it can be easily concluded that fibers with higher aspect ratios increase the compressive strength of GFRGC at a lower volume fraction with the addition of glass fibers, whereas glass fibers with lower aspect ratios increase the compressive strength of GFRGC at a higher volume fraction with the addition of glass fibers [136,139]. Figure 11 depicts what glass fibers look like. Table 4 includes the literature survey on GFRGC.

Figure 11. Glass fibers. Reprinted/adapted with permission from Ref. [140], 2019, Elsevier Ltd. All rights reserved. Selection and peer-review under responsibility of scientific committee of Innovative Advancement in Engineering & Technology.

Table 3. Details of different types of glass fibers.

Fiber Type	Aspect Ratio	Elastic Modulus (MPa)	Strength (MPa)	Density kg/m^3	Reference
Glass fiber	600	82,000	2500	2540	[136]
Alkali-resistant glass fiber	928.5	-	-	2650	[137]
Alkali and acid resistant glass fiber	60	72,000	1700	-	[138]
Glass fiber (Domcrete Australia)	135	70,000	-	-	[141]
Glass fiber (Type A)	35	42,000	>1000	-	[139]
Glass fiber (Type B)	62	42,000	>1000	-	[139]
E-glass fiber	-	72,300	3445	2580	[142]

Table 4. Literature survey on GFRGC.

Reference	Precursor Type	Activator Type	Molarity	Fiber Content	Aspect Ratio	Curing Type	Effect
[137]	Fly ash (Class F)	NaOH + Na_2SiO_3	8 M	0%, 0.50%, 0.75%, 1.00%, and 1.25% (by volume fraction)	928.57	Heat curing	Fiber addition decreases the workability and increases the density. The increase in the fiber content leads to the increase in the compressive and flexural strengths. 1.25% is the optimum fiber content.
[136]	Fly ash (Class F)	NaOH + Na_2SiO_3	12 M, 16 M, 20 M	0%, 0.1%, 0.2%, 0.3%, 0.4%, and 0.5% (by volume fraction)	600	Ambient curing, Heat curing	Molarity affects the mechanical properties of concrete. Maximum compressive, tensile, and flexural strengths were achieved with 16 M alkaline solution. 0.3% was found to be the optimum fiber content. Heat-cured specimens exhibited higher strength in comparison to ambient-cured specimens.
[140]	Fly ash (Class F)	NaOH + Na_2SiO_3	14 M	0.15%, 0.3%, and 0.5% (by volume fraction)	1000	Heat curing	Maximum compressive strength was obtained for the specimen with 0.5% glass fibers (for example, 15% more than conventional). In comparison to the steel fiber specimen, the glass fiber specimen demonstrated higher mechanical strength increment.

Table 4. *Cont.*

Reference	Precursor Type	Activator Type	Molarity	Fiber Content	Aspect Ratio	Curing Type	Effect
[134]	Fly ash (Class F)	NaOH + Na_2SiO_3	14 M	0%, 0.5%, 1.0%, 1.5%, 2.0%, and 2.5% (by volume fraction)	-	Heat curing (varying)	Maximum strengths (compressive, splitting tensile, and flexural stengths) were obtained with 2% glass fibers by volume fraction at 60 °C. Effective mechanical properties can be obtained utilizing eco-friendly materials, for example, geopolymer.
[133]	Fly ash GGBS Condensed silica fume Metakaolin	NaOH + Na_2SiO_3	8 M	0.50%, 0.75%, and 1.0% (by volume fraction)	860	Ambient curing	60% GGBS, 30% fly ash, 5% condensed silica fume, and 5% metakaolin were found to be the most effective combination of precursors for the strength increment. The addition of glass fibers helps in arresting microcracks that make geopolymer concrete ductile. Specimens if cured for a longer period in ambient temperature, would enhance the strength properties of GFRGC. 1% glass fibers when incorporated in the above mentioned precursor combination revealed the maximum strength.
[135]	Fly ash (Class F)	NaOH + Na_2SiO_3	10 M	1% micro glass fiber with varying dosages of nano $CaCO_3$ (1%, 2%, and 3%) (by volume fraction)	NA	Heat curing	2% nano $CaCO_3$ along with 1% micro glass fibers can enhance the mechanical properties of FRGC. Incorporation of calcium carbonate tends to refine the microstructure and interfacial zones in addition to the acceleration of the geopolymerization reaction.
[143]	Fly ash (Class F)	NaOH + Na_2SiO_3	14 M	0%, 0.5%, 1%, 1.5%, and 2.0% (by volume fraction)	NA	Heat curing	The analysis was carried out using glass fibers, and sand was replaced with copper slag. 2% was the optimum fiber content. Results for the mechanical strengths (compressive, splitting, and flexural stengths) were maximum for the optimum content.
[144]	Fly ash (Class F)	NaOH + Na_2SiO_3	14 M	0.3%, 1%, 2%, 3%, and 3.5% (by weight)	NA	Heat curing	3% glass fibers by weight when incorporated in concrete improved the compressive strength along with a positive change in the flexural strength. The optimum ratio of sodium silicate and caustic soda was found to be 1.5 for the maximum compressive strength.

4.3. Polypropylene Fiber

In recent years, the use of fibers named polypropylene in plain concrete has gained popularity. Further, the use of the fibers in plain concrete improves the crack resistance and reduces the shrinkage [145]. To enhance the compressive strength of polypropylene fiber-reinforced geopolymer concrete (PPFRGC) in comparison to plain concrete, it is necessary to ensure the optimum amount of fibers to be added. Reed et al. [145] recommended that 0.05% (added by weight) polypropylene fibers was the optimum content, as it indicates the best compressive strength result for all testing days (specimen testing was carried out for 0, 10, 20, 30, 40, 50, and 60 days). Also, due to the random distribution, polypropylene fibers limit the propagation of cracks. Ranjbar et al. [146] discussed the long-term effect of polypropylene fibers on increasing the compressive strength. It was resulted that no significant increase in the compressive strength was witnessed at the early ages, but the addition of polypropylene fibers adversely affected the concrete's compressive strength. Moreover, higher energy absorption up to 3% polypropylene fibers was observed (from 2.5% to 5% higher compared to the geopolymer specimen with no fiber). Rajak and Rai [147] stated that the loss in the compressive strength for PPFRGC specimens was evidenced when oven cured at 80 °C for 24 h. The loss in the compressive strength decreased with increasing the content of polypropylene fibers with a minimum 5% loss at 0.2% fiber inclusion. Aygörmez et al. [148] performed research on PPFRGC with polypropylene fibers of higher strength and higher aspect ratio. The research was conducted to acknowledge the effects of higher temperatures (for example, 300 °C, 600 °C, and 900 °C). The compressive strength decreased considerably when the temperature increased beyond 600 °C. Figure 12 displays a field emission scanning electron microscope (FESEM) image that provides a detailed view of the surface morphology of polypropylene fibers. Figure 13 illustrates a FESEM image that depicts the interaction between the fibers and matrix material within the examined specimen.

Table 5 presents details of various types of polypropylene fibers used in experimental investigations of PPFRGC by several researchers. Comparing the studies done by Ranjbar et al. [146] and Aygörmez et al. [148], the former suggested that the addition of polypropylene fibers to fly ash-based geopolymer concrete had mixed effects. Polypropylene fibers, due to their hydrophobic nature, exhibited weak initial bonding with the binder and eventually led to debonding over time, resulting in reduced flexural strength. However, it improved the energy absorption compared to the fiberless geopolymer paste. In contrast, the incorporation of micro steel fibers enhanced the energy absorption and flexural strength and reduced the shrinkage without noticeably affecting the compressive strength. The study emphasized the importance of considering both fiber–matrix interaction and binder shrinkage for the evaluation of FRGC. Whereas the latter highlighted that the inclusion of polypropylene fibers in geopolymer matrices, along with colemanite waste and silica fume substitution, yielded slight enhancements in the composite's performance. Polypropylene fibers helped increase the residual compressive and flexural strengths, especially under high-temperature conditions (from 600 °C to 900 °C). The use of air-entraining admixture, however, negatively impacted the strength results. Additionally, the freezing-thawing test showed fluctuations in the compressive strength, ultrasonic pulse velocity, and weight changes, which are attributed to the severity of the regime and affect the integrity of the composite materials over service conditions. Table 6 provides the literature survey on PPFRGC.

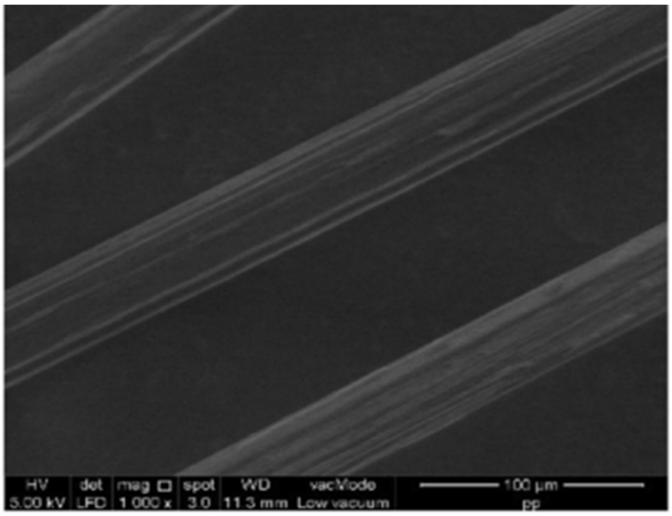

Figure 12. FESEM image of surface morphology of polypropylene fibers. Reprinted/adapted with permission from Ref. [146], 2015, Elsevier Ltd. All rights reserved.

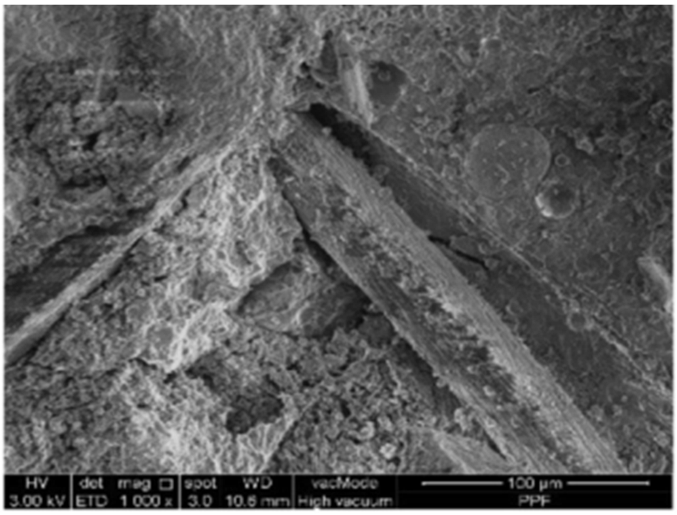

Figure 13. FESEM image showing fibers–matrix interaction. Reprinted/adapted with permission from Ref. [146], 2015, Elsevier Ltd. All rights reserved.

Table 5. Details of different types of polypropylene fibers.

Fiber Type	Aspect Ratio	Modulus of Elasticity (MPa)	Strength (MPa)	Density (g/cm^3)	Reference
Polypropylene fiber	171.42	3500	400	9.10	[112]
Crimped polypropylene fiber	76.47	3000	250	9.05	[117]
Polypropylene fiber	300	3500	310	9.05	[146]
Micro polypropylene fiber	3750	3000	-	9.10	[147]
Polypropylene fiber	923	4200	350	9.10	[149]
Polypropylene fiber	1600	-	750	9.10	[148]

Table 6. Literature survey on PPFRGC.

Reference	Precursor Type	Activator Type	Molarity	Fiber Content	Aspect Ratio	Curing Type	Effect
[145]	Fly ash (Class F)	NaOH + Na_2SiO_3	8 M	0%, 0.05%, and 0.15%	-	Heat curing, Ambient curing	Improved compressive strength and ductility. No effect of curing on the compressive strength. Maximum strength of specimens was at 21 and 28 days of testing.
[146]	Fly ash (Class F)	NaOH + Na_2SiO_3	16 M	0%, 0.5%, 1.0%, 2.0%, 3.0%, and 4.0% (by volume fraction)	300	Heat curing	0.50% polypropylene fibers demonstrated the compressive strength increment at 7 days of curing, which was further decreased. In the long term, the strength of geopolymer composite decreased with the increase in the polypropylene fiber content. Also, polypropylene fibers exhibited hydrophobic characteristics.
[147]	Fly ash (Class F)	NaOH + Na_2SiO_3	14 M	0%, 0.1%, 0.15%, 0.20%, 0.25%, 0.30%, 0.40%, and 0.50% (by volume fraction)	375	Heat curing	Polypropylene fibers indicated a large effect on the splitting tensile strength of geopolymer concrete when compared to the conventional geopolymer concrete, while gave no positive effect on the compressive strength. Failure pattern changed from brittle to ductile. Reduction in the capillary porosity was obtained when polypropylene fibers were used in geopolymer concrete, which was favorable to the durability.
[150]	Fly ash (Class F) and wood ash	NaOH + Na_2SiO_3	10 M	0%, 0.5%, 1.0%, 1.5%, and 2.0% (by volume fraction)	200	Ambient curing	With an increase in the molarity up to 13 M, there was a gradual increase in the compressive strength. 10 M was taken as the optimum for further experimental investigations. 1% polypropylene fibers increased the mechanical strength of geopolymer concrete, beyond 1% polypropylene fibers there was a decline in the mechanical strength.
[149]	Fly ash	NaOH + Na_2SiO_3	12 M 14 M 16 M	0%, 0.5%, and 1.0% (by volume fraction)	923	Ambient curing	16 M provided the best alkaline condition for geopolymerization. Good mechanical performance, high viscosity, and good adherence were acknowledged after the incorporation of polypropylene fibers in geopolymer concrete.

Table 6. *Cont.*

Reference	Precursor Type	Activator Type	Molarity	Fiber Content	Aspect Ratio	Curing Type	Effect
[148]	Metakaolin, silica fume, slag, and colemanite	NaOH + Na_2SiO_3	12 M	0.8% (by volume fraction)	1600	Heat curing (varying temperatures)	There was a decrease in the flexural and compressive strengths at elevated temperatures ranging between 600 °C and 900 °C. This was mainly owing to fibers and dehydration melting of the geopolymer matrix. There was a slight improvement in the properties of PPFRGC.
[151]	Fly ash	NaOH + Na_2SiO_3	10 M	0%, 0.52%, 1.04%, and 1.56% (by volume fraction)	666.6	Ambient curing	0.52% was the optimum polypropylene fiber content for the compressive strength and 1.04% was the optimum polypropylene fiber content for the flexural strength. The mechanical strength of PPFRGC was adversely affected by the elevated temperatures, due to the weight loss of the paste as there was an increase in the large capillary pores and air voids.
[152]	Fly ash (Class C)	NaOH + Na_2SiO_3	10 M	0%, 0.5%, 1.0%, and 1.5% (by weight)	666.6	Ambient curing	Thermal conductivity of geopolymer concrete was not affected by the addition of polypropylene fibers. There was no positive effect of polypropylene fibers on the compressive strength of geopolymer concrete.

4.4. Basalt Fiber

Basalt fibers are obtained from a fine-grained solidified volcanic stone, which are commonly recognized as basalt [153,154]. Volcanic magma (a very hot fluid beneath the earth's crust that solidifies when exposed to open air) is the source of origin of basalt. Basalt, due to its application as a paving and building stone in its natural form, is known from the Roman age [154]. In 1923, the French Paul Dhé received a US patent for his idea to extrude fibers from basalt [155]. From the 1960s, just after World War II, basalt fibers were chosen to be the best material for military research by the Soviet Union, Europe, and the United States due to their extensive use in aeronautical and defense applications [144,146]. In 1995, the fiber production technology was declassified and commenced civilian research [155]. The extrusion of basalt fibers is carried out generally by melting the basalt rock at a temperature of approximately 1400 °C in a fine fiber from 0.009 mm to 0.013 mm in diameter [154,156]. The addition of 2% basalt fibers to fly ash and GGBS-based geopolymer composite increases its compressive strength and splitting tensile strength. There was a 10% immediate increase in the strength for the specimen with 0.5% basalt fibers cured for 7 days compared to the reference specimen. However, in the specimens cured for 28 days, the strength increased by 10%, 17%, 25%, and 34% having 0.5%, 1.0%, 1.5%, and 2.0% basalt fibers, respectively [157]. Taking the length of basalt fibers into consideration, there were some variations in the strength among different basalt fiber lengths. In addition, 0.1% basalt fibers with the length of 6 mm, when incorporated in geopolymer composite, gave the best result in the compressive strength compared to basalt fibers with the lengths of 3 mm, 12 mm, and 18 mm. Furthermore, the inclusion of basalt fibers demonstrated its effect on the fracture process of fly ash geopolymer concrete. The addition of basalt fibers to fly ash geopolymer concrete leads to linear elastic deformation at the initial loading stage, whereas it results in nonlinear deformation along with microcracks with increasing the load. Also, the inclusion of basalt fibers in fly ash geopolymer concrete affects the fracture toughness and fracture energy [158]. Temuujin et al. [159] explained that basalt fiber coating is a prime factor that influences the strength of basalt fiber-reinforced geopolymer concrete (BFRGC). Spooled fibers coated with a carbon layer illustrated the best bonding between the fibers and polymer matrix compared to the chopped fibers.

Details of basalt fibers such as aspect ratio, modulus of elasticity, strength, and density are listed in Table 7 from various literatures. After conducting the literature survey, it was concluded that very few experimental investigations have been done using basalt fibers in geopolymer concrete. From the available literature mentioned in this review article, it was found that the aspect ratio ranges from 600 to 2500, the modulus of elasticity ranges from 75 MPa to 110 MPa, fiber strength ranges from 1450 MPa to 4100 MPa, and the density of basalt fibers ranges from 2630 kg/m^3 to 2660 kg/m^3. Considering Tables 1, 3, 5 and 7, the strength of polypropylene fibers compared to steel fibers, glass fibers, and basalt fibers was less and ranged between 250 MPa and 750 MPa. Ronad et al. [157] reported a notable 34.74% increase in the compressive strength with the fiber incorporation, pointing out their effectiveness as crack arrestors. Wang et al. [158] corroborates these findings, emphasizing the substantial improvements in the compressive and splitting tensile strengths. Therefore, it can be concluded that the addition of basalt fibers to geopolymer concrete greatly improves its mechanical properties. Table 8 consists of the literature survey on BFRGC.

Table 7. Details of different types of basalt fibers.

Fiber Type	Aspect Ratio	Modulus of Elasticity (MPa)	Strength (MPa)	Density (kg/m^3)	Reference
Basalt fiber	-	75–90 GPa	3200–3850	2630	[157]
Basalt fiber (straight)	2500	89 GPa	1680	2660	[160]
Basalt fiber	-	88 GPa	1450	2630	[158]
Basalt fiber	1000	110 GPa	3200	-	[161]
Basalt fiber	600	88 GPa	4100	-	[162]

Table 8. Literature survey on BFRGC.

Reference	Precursor Type	Activator Type	Molarity	Fiber Content	Aspect Ratio	Curing Type	Effect
[157]	Fly ash (Class F) + GGBS	NaOH + Na_2SiO_3	10 M	0%, 0.5%, 1.0%, 1.5%, 2.0%, and 2.5% (by weight of cementitious material)		Ambient curing	Increase in the basalt fiber content in geopolymer concrete by up to 2.0% enhanced the mechanical properties (for example, the compressive and tensile strengths) of BFRGC. Therefore, 2.0% was found to be the optimum basalt fiber content for BFRGC.
[160]	Fly ash (Class C)	NaOH + Na_2SiO_3	5 M	0.038%, 0.095%, and 0.19% (by volume fraction)	2500	Ambient curing	Basalt fibers in geopolymer concrete displayed a slight improvement in the mechanical strength for the volume fraction in the ranged from 0.038% to 0.91%. 0.095% was the optimum fiber content. Basalt fibers in geopolymer concrete noticeably influenced the geoplomer concrete's fracture property. Consequently, it was proven that geopolymer concrete with basalt fibers can resist cracks.
[159]	Fly ash	NaOH + Na_2SiO_3	8 M	1% (chopped fiber, 2 cm in length) 1% (spooled fiber, 6 mm in length)	2000 to 2858 (for chopped fiber)	Heat curing	Strength of the geopolymer concrete paste decreased with the inclusion of 1% basalt fibers in the geopolymer concrete paste. The strength of the geopolymer concrete paste with spooled basalt fibers was better compared to chopped basalt fibers. Better adhesion was achieved between the geopolymer concrete paste and basalt fibers for spooled basalt fibers coated with a carbon layer. Also, it exhibited better performance against the alkaline solution.
[158]	Fly ash (Class F)	NaOH + Na_2SiO_3	NA	1% (by volume fraction)	Varying for different lengths (for example, 3, 6, 12, and 18 (in mm)	Heat curing	Basalt fibers in geopolymer concrete improved the mechanical properties. 1% of 6 mm basalt fibers when incorporated in geopolymer concrete indicated the best result among all other tested specimens, whether fiber reinforced or plain. Incorporation of basalt fibers decreased the crack length of BFRGC, and the most prominent fiber length was found to be 6 mm.

Table 8. *Cont.*

Reference	Precursor Type	Activator Type	Molarity	Fiber Content	Aspect Ratio	Curing Type	Effect
[163]	Fly ash (Class F)	KOH + K_2SiO_3	8 M	0%, 0.5%, 1.0%, and 1.5%	977	Heat curing	1% was the optimum basalt fiber content. Basalt fibers in geopolymer concrete at elevated temperatures (up to 600 °C) lowered the mass loss and volumetric shrinkage and improved the compressive strength of BFRGC.
[161]	Rice husk ash (RHA)	NaOH + Na_2SiO_3	14 M	0%, 1%, 5%, 10%, 15%, 20%, and 25% (replacement was carried out with RHA)	1000	Ambient curing	By replacing basalt fibers with RHA, the modulus of elasticity of the specimen was increased with the increase in the density of RHA-based fiber specimen. The optimum results were achieved for 10% basalt fiber replacement with RHA. Poisson's ratio decreased with an increment in the basalt fiber content. Maximum flexural strength was obtained for the specimen having 10% basalt fiber replacement with RHA.
[162]	Metakaolin + GGBS	NaOH + Na_2SiO_3	12 M	0%, 0.4%, 0.8%, and 1.26% (by volume fraction)	600	Heat curing	The mechanical and physical properties of the composite were found to be excellent after the incorporation of basalt sand. Also, the use of basalt fibers enhanced the properties of geopolymer concrete. The negative effect of the elevated temperatures beyond 800 °C on BFRGC was observed.

5. Conclusions

Geopolymers exhibit brittle failures and weak tension. To overcome these failures and weaknesses, numerous studies have concentrated on the inclusion of various fibers in geopolymer to achieve ideal mechanical and thermal qualities for each individual application. This article highlighted numerous issues, recent discoveries, and potential uses for FRGCs. Different types of fibers, including synthetic, organic, inorganic, and natural fibers, are considered for reinforcement in the geopolymer matrix. Additionally, one of the latest approaches for enhancing the mechanical strength of the fibers in geopolymer composites is hybrid fiber reinforcement. Achieving a strong bond between the fibers and geopolymer matrix in concrete involves careful consideration of material selection, mixture design, and environmental conditions. By optimizing these key factors, engineers can improve the performance of geopolymer concrete in various applications. The current review article investigated how a combination of hybrid fibers and other types of fiber reinforcements affect the composite's overall performance. Applications for geopolymer span a broad spectrum, from basic building to cutting-edge foams and thermal insulators. The conclusions for different types of the fibers are provided below:

- Steel fibers, with their diverse types and properties, play a crucial role in enhancing the performance of concrete composites. SFRC finds wide applications in civil engineering such as improving the toughness, impact resistance, and abrasion resistance. The addition of steel fibers reduces sorptivity and enhances durability, while alumina-coated steel fibers significantly improve the interfacial bond strength and mechanical behavior in polymer composites. Also, elevated temperatures impact SFRGC, with an initial strength improvement up to 400 °C, followed by a decreasing strength.
- Glass fibers, including CR, E-glass, and HS types, are commonly utilized to reinforce polymers. HS glass fibers exhibit superior creep and fatigue resistance compared to E-glass fibers. Glass fibers improve the density, ductility, and crack resistance of geopolymer concrete. Incorporating nano $CaCO_3$ enhances the compressive strength, and the higher NaOH molarity leads to improved mechanical performance. The addition of glass fibers affects the workability and density negatively, but remarkably enhances the impact strength due to the increased elasticity and stiffness.
- The polypropylene fiber's application in plain concrete has gained popularity for increasing the crack resistance and reducing the shrinkage. Research suggests that an optimal addition of 0.05% polypropylene fibers by weight improves the compressive strength. Meanwhile, the polypropylene fiber's random distribution limits the crack propagation. However, high-temperature exposure, such as 600 °C and 900 °C, significantly reduces the compressive strength in PPFRGC.
- Basalt fibers, originating from a solidified volcanic stone, have a rich history, known since the Roman times for their natural applications in construction. Their industrial use began in 1923 with a US patent and gained prominence post-World War II for military and aerospace applications. By 1995, civilian research commenced, utilizing extrusion techniques at 1400 °C. Incorporating basalt fibers increases the strength of geopolymer composites, with varying effects based on the fibers' length. In addition, they influence the fracture behavior and bonding with the polymer matrix, with carbon-coated spooled fibers showing superior performance.

Author Contributions: U.S.: conceptualization, methodology, investigation, validation, writing—original draft. N.G.: conceptualization, methodology, investigation, validation, writing—original draft. A.B.: conceptualization, methodology, investigation, validation, formal analysis, resources, writing—original draft, writing—review and editing. Y.O.Ö.: conceptualization, methodology, investigation, validation, writing—original draft, writing—review and editing. M.V.: conceptualization, methodology. P.B.: methodology, investigation. E.A.: investigation, validation. S.I.: investigation, formal analysis. M.A.K.: validation, formal analysis. All authors have read and agreed to the published version of the manuscript.

Funding: This research received no external funding.

Data Availability Statement: Not applicable.

Acknowledgments: The authors extend their appreciation to the Deanship of Scientific Research at King Khalid University, Abha, Saudi Arabia for providing financial support to this research work through Large Groups Research Project under grant number RGP2/563/44.

Conflicts of Interest: The author, Ujjwal Sharma, was employed by the company Ixrlabs Learning Solutions Pvt. Ltd. The remaining authors declare that the research was conducted in the absence of any commercial or financial relationships that could be construed as a potential conflict of interest.

References

1. Banks, A.S.; Carr, D.L. Urbanization; modernization: A longitudinal analysis. *Stud. Comp. Int. Dev.* **1974**, *9*, 26–45. [CrossRef] [PubMed]
2. Ritchie, H.; Roser, M. Urbanization-Our World in Data, Our World in Data. 2018. Available online: https://ourworldindata.org/urbanization (accessed on 17 December 2022).
3. Jahami, A.; Issa, C.A. Exploring the use of mixed waste materials (MWM) in concrete for sustainable construction: A review. *Constr. Build Mater.* **2023**, *398*, 132476. [CrossRef]
4. Zhou, F.; Li, W.; Hu, Y.; Huang, L.; Xie, Z.; Yang, J.; Wu, D.; Chen, Z. Moisture diffusion coefficient of concrete under different conditions. *Buildings* **2023**, *13*, 2421. [CrossRef]
5. Aprianti, E. A huge number of artificial waste material can be supplementary cementitious material (SCM) for concrete production—A review part II. *J. Clean Prod.* **2017**, *142*, 4178–4194. [CrossRef]
6. Shafigh, P.; Mahmud, H.B.; Jumaat, M.Z.; Zargar, M. Agricultural wastes as aggregate in concrete mixtures—A review. *Constr. Build Mater.* **2014**, *53*, 110–117. [CrossRef]
7. Goyal, A.; Palaia, I.; Ioannidou, K.; Ulm, F.J.; van Damme, H.; Pellenq, R.J.M.; Trizac, E.; Del Gado, E. The physics of cement cohesion. *Sci. Adv.* **2021**, *7*, eabg5882. [CrossRef]
8. Topark-Ngarm, P.; Chindaprasirt, P.; Sata, V. Setting time, strength, and bond of high-calcium fly ash geopolymer concrete. *J. Mater. Civ. Eng.* **2015**, *27*, 04014198. [CrossRef]
9. US Geological Survey. *Mineral Commodity Summaries*; US Geological Survey: Reston, VA, USA, 2022.
10. Bekun, F.V.; Alola, A.A.; Gyamfi, B.A.; Kwakwa, P.A.; Uzuner, G. Econometrics analysis on cement production and environmental quality in European Union countries. *Int. J. Environ. Sci. Technol.* **2023**, *20*, 4265–4280. [CrossRef]
11. Özkılıç, Y.O.; Zeybek, Ö.; Bahrami, A.; Celik, A.I.; Mydin, M.A.O.; Karalar, M.; Hakeem, I.Y.; Roy, K.; Jagadesh, P. Optimum usage of waste marble powder to reduce use of cement toward eco-friendly concrete. *J. Mater. Res. Technol.* **2023**, *25*, 4799–4819. [CrossRef]
12. Gerges, N.; Issa, C.A.; Antoun, M.; Sleiman, E.; Hallal, F.; Shamoun, P.; Hayek, J. Eco-friendly mortar: Optimum combination of wood ash, crumb rubber, and fine crushed glass. *Case Stud. Constr. Mater.* **2021**, *15*, e00588. [CrossRef]
13. Çelik, A.İ.; Özkılıç, Y.O.; Bahrami, A.; Hakeem, I.Y. Effects of glass fiber on recycled fly ash and basalt powder based geopolymer concrete. *Case Stud. Constr. Mater.* **2023**, *19*, e02659. [CrossRef]
14. Waqas, H.A.; Bahrami, A.; Sahil, M.; Poshad Khan, A.; Ejaz, A.; Shafique, T.; Tariq, Z.; Ahmad, S.; Özkılıç, Y.O. Performance prediction of hybrid bamboo-reinforced concrete beams using gene expression programming for sustainable construction. *Materials* **2023**, *16*, 6788. [CrossRef]
15. Gerges, N.N.; Issa, C.A.; Sleiman, E.; Aintrazi, S.; Saadeddine, J.; Abboud, R.; Antoun, M. Eco-friendly optimum structural concrete mix design. *Sustainability* **2022**, *14*, 8660. [CrossRef]
16. Çelik, A.İ.; Özkılıç, Y.O.; Bahrami, A.; Hakeem, I.Y. Mechanical performance of geopolymer concrete with micro silica fume and waste steel lathe scraps. *Case Stud. Constr. Mater.* **2023**, *19*, e02548. [CrossRef]
17. Ahmad, S.; Dawood, O.; Lashin, M.M.; Khattak, S.U.; Javed, M.F.; Aslam, F.; Khan, M.I.; Elkotb, M.; Alaboud, T.M. Effect of coconut fiber on low-density polyethylene plastic-sand paver blocks. *Ain Shams Eng. J.* **2023**, *14*, 101982. [CrossRef]
18. Kim, Y.Y.; Lee, B.J.; Saraswathy, V.; Kwon, S.J. Strength and durability performance of alkali-activated rice husk ash geopolymer mortar. *Sci. World J.* **2014**, *2014*, 209584. [CrossRef] [PubMed]
19. Ramadan, R.; Jahami, A.; Khatib, J.; El-Hassan, H.; Elkordi, A. Improving structural performance of reinforced concrete beams with Phragmites australis fiber and waste glass additives. *Appl. Sci.* **2023**, *13*, 4206. [CrossRef]
20. Gerges, N.N.; Issa, C.A.; Khalil, N.J.; Abdul Khalek, L.; Abdo, S.; Abdulwahab, Y. Flexural capacity of eco-friendly reinforced concrete beams. *Sci. Rep.* **2023**, *13*, 20142. [CrossRef] [PubMed]
21. Antoun, M.; Issa, C.A.; Aouad, G.; Gerges, N. Sustainable masonry blocks: Olive wood waste as substitute for fine aggregates. *Case Stud. Constr. Mater.* **2021**, *15*, e00590. [CrossRef]
22. Aksoylu, C.; Özkılıç, Y.O.; Bahrami, A.; Yıldızel, S.A.; Hakeem, I.Y.; Özdöner, N.; Basaran, B.; Karalar, M. Application of waste ceramic powder as a cement replacement in reinforced concrete beams toward sustainable usage in construction. *Case Stud. Constr. Mater.* **2023**, *19*, e02444. [CrossRef]
23. Alola, A.A.; Bekun, F.V.; Adebayo, T.S.; Uzuner, G. The nexus of disaggregated energy sources and cement production carbon mission in China. *Energy Environ.* **2022**, *34*, 1937–1956. [CrossRef]
24. Andrew, R.M. Global CO_2 emissions from cement production. *Earth Syst. Sci. Data* **2018**, *10*, 195–217. [CrossRef]

25. Dindi, A.; Quang, D.V.; Vega, L.; Nashef, E.; Abu-Zahra, M.R.M. Applications of fly ash for CO_2 capture, utilization, and storage. *J. CO2 Util.* **2019**, *29*, 82–102. [CrossRef]
26. Worrell, E.; Price, L.; Martin, N.; Hendriks, C.; Meida, L.O. Carbon dioxide emissions from the global cement industry. *Annu. Rev. Energy Environ.* **2001**, *26*, 303–329. [CrossRef]
27. Zakka, W.P.; Lim, N.H.A.S.; Khun, M.C. A scientometric review of geopolymer concrete. *J. Clean Prod.* **2021**, *280*, 124353. [CrossRef]
28. Serdar, M.; Bjegovic, D.; Stirmer, N.; Pecur, I.B. Alternative binders for concrete: Opportunities and challenges. *Gradevinar* **2019**, *71*, 200–218. [CrossRef]
29. Ismail, I.; Bernal, S.A.; Provis, J.L.; Nicolas, R.S.; Hamdan, S.; Van Deventer, J.S.J. Modification of phase evolution in alkali-activated blast furnace slag by the incorporation of fly ash. *Cem. Concr. Compos.* **2014**, *45*, 125–135. [CrossRef]
30. Juenger, M.C.G.; Winnefeld, F.; Provis, J.L.; Ideker, J.H. Advances in alternative cementitious binders. *Cem. Concr. Res.* **2011**, *41*, 1232–1243. [CrossRef]
31. Zeyad, A.M.; Johari, M.A.M.; Abutaleb, A.; Tayeh, B.A. The effect of steam curing regimes on the chloride resistance and pore size of high–strength green concrete. *Constr. Build Mater.* **2021**, *280*, 122409. [CrossRef]
32. Huang, H.; Guo, M.; Zhang, W.; Huang, M. Seismic behavior of strengthened RC columns under combined loadings. *J. Bridge Eng.* **2022**, *27*, 05022005. [CrossRef]
33. Abdal, S.; Mansour, W.; Agwa, I.; Nasr, M.; Abadel, A.; Özkılıç, Y.O.; Akeed, M.H. Application of ultra-high-performance concrete in bridge engineering: Current status, limitations, challenges, and future prospects. *Buildings* **2023**, *13*, 185. [CrossRef]
34. Huang, H.; Li, M.; Zhang, W.; Yuan, Y. Seismic behavior of a friction-type artificial plastic hinge for the precast beam–column connection. *Arch. Civ. Mech. Eng.* **2022**, *22*, 201. [CrossRef]
35. Meskhi, B.; Beskopylny, A.N.; Stel'makh, S.A.; Shcherban', E.M.; Mailyan, L.R.; Shilov, A.A.; El'shaeva, D.; Shilova, K.; Karalar, M.; Özkılıç, Y.O. Analytical review of geopolymer concrete: Retrospective and current issues. *Materials* **2023**, *16*, 3792. [CrossRef] [PubMed]
36. Liu, C.; Cui, J.; Zhang, Z.; Liu, H.; Huang, X.; Zhang, C. The role of TBM asymmetric tail-grouting on surface settlement in coarse-grained soils of urban area: Field tests and FEA modelling. *Tunn. Undergr. Space Technol.* **2021**, *111*, 103857. [CrossRef]
37. Jin, M.; Ma, Y.; Li, W.; Huang, J.; Yan, Y.; Zeng, H.; Lu, C.; Liu, J. Multi-scale investigation on composition-structure of C-(A)-S-H with different Al/Si ratios under attack of decalcification action. *Cem. Concr. Res.* **2023**, *172*, 107251. [CrossRef]
38. Chang, Q.; Liu, L.; Farooqi, M.U.; Thomas, B.; Özkılıç, Y.O. Data-driven based estimation of waste-derived ceramic concrete from experimental results with its environmental assessment. *J. Mater. Res. Technol.* **2023**, *24*, 6348–6368. [CrossRef]
39. Sun, L.; Wang, C.; Zhang, C.; Yang, Z.; Li, C.; Qiao, P. Experimental investigation on the bond performance of sea sand coral concrete with FRP bar reinforcement for marine environments. *Adv. Struct. Eng.* **2022**, *26*, 533–546. [CrossRef]
40. Wang, M.; Yang, X.; Wang, W. Establishing a 3D aggregates database from X-ray CT scans of bulk concrete. *Constr. Build. Mater.* **2022**, *315*, 125740. [CrossRef]
41. He, H.; Shuang, E.; Wen, T.; Yao, J.; Wang, X.; He, C.; Yu, Y. Employing novel N-doped graphene quantum dots to improve chloride binding of cement. *Constr. Build. Mater.* **2023**, *401*, 132944. [CrossRef]
42. Lin, T.S.; Jia, D.C.; He, P.G.; Wang, M.R. Thermal-mechanical properties of short carbon fiber reinforced geopolymer matrix composites subjected to thermal load. *J. Cent. South Univ. Technol. Engl. Ed.* **2009**, *16*, 881–886. [CrossRef]
43. Zhou, S.; Lu, C.; Zhu, X.; Li, F. Preparation and characterization of high-strength geopolymer based on BH-1 lunar soil simulant with low alkali content. *Engineering* **2021**, *7*, 1631–1645. [CrossRef]
44. Li, Z.; Gao, M.; Lei, Z.; Tong, L.; Sun, J.; Wang, Y.; Wang, X.; Jiang, X. Ternary cementless composite based on red mud, ultra-fine fly ash, and GGBS: Synergistic utilization and geopolymerization mechanism. *Case Stud. Constr. Mater.* **2023**, *19*, e2410. [CrossRef]
45. Papakonstantinou, C.G.; Balaguru, P.; Lyon, R.E. Comparative study of high temperature composites. *Compos. Part B Eng.* **2001**, *32*, 637–649. [CrossRef]
46. Barbosa, V.F.F.; MacKenzie, K.J.D. Synthesis and thermal behaviour of potassium sialate geopolymers. *Mater. Lett.* **2003**, *57*, 1477–1482. [CrossRef]
47. Yip, C.K.; Lukey, G.C.; Provis, J.L.; van Deventer, J.S.J. Effect of calcium silicate sources on geopolymerisation. *Cem. Concr. Res.* **2008**, *38*, 554–564. [CrossRef]
48. Palomo, A.; Grutzeck, M.W.; Blanco, M.T. Alkali-activated fly ashes: A cement for the future. *Cem. Concr. Res.* **1999**, *29*, 1323–1329. [CrossRef]
49. Van Deventer, J.S.J.; Provis, J.L.; Duxson, P.; Lukey, G.C. Reaction mechanisms in the geopolymeric conversion of inorganic waste to useful products. *J. Hazard. Mater.* **2007**, *139*, 506–513. [CrossRef]
50. Yang, H.; Liu, L.; Yang, W.; Liu, H.; Ahmad, W.; Ahmad, A.; Aslam, F.; Joyklad, P. A comprehensive overview of geopolymer composites: A bibliometric analysis and literature review. *Case Stud. Constr. Mater.* **2022**, *16*, e00830. [CrossRef]
51. Almutairi, A.L.; Tayeh, B.A.; Adesina, A.; Isleem, H.F.; Zeyad, A.M. Potential applications of geopolymer concrete in construction: A review. *Case Stud. Constr. Mater.* **2021**, *15*, e00733. [CrossRef]
52. Shamsaei, E.; Bolt, O.; de Souza, F.B.; Benhelal, E.; Sagoe-Crentsil, K.; Sanjayan, J. Pathways to commercialisation for brown coal fly ash-based geopolymer concrete in Australia. *Sustainability* **2021**, *13*, 4350. [CrossRef]
53. Thomas, B.S.; Yang, J.; Mo, K.H.; Abdalla, J.A.; Hawileh, R.A.; Ariyachandra, E. Biomass ashes from agricultural wastes as supplementary cementitious materials or aggregate replacement in cement/geopolymer concrete: A comprehensive review. *J. Build. Eng.* **2021**, *40*, 102332. [CrossRef]

54. Tayeh, B.A.; Zeyad, A.M.; Agwa, I.S.; Amin, M. Effect of elevated temperatures on mechanical properties of lightweight geopolymer concrete. *Case Stud. Constr. Mater.* **2021**, *15*, e00673. [CrossRef]
55. Huang, H.; Yuan, Y.; Zhang, W.; Zhu, L. Property assessment of high-performance concrete containing three types of fibers. *Int. J. Concr. Struct. Mater.* **2021**, *15*, 39. [CrossRef]
56. Dang, J.; Shen, X.; Castel, A.; Aldred, J. Monitoring apparent pH value in geopolymer concrete using glass electrode. In Proceedings of the ISARC 2016—33rd International Symposium on Automation and Robotics in Construction, Auburn, AL, USA, 18–21 July 2016. [CrossRef]
57. Çelik, A.İ.; Tunç, U.; Bahrami, A.; Karalar, M.; Mydin, M.A.O.; Alomayri, T.; Özkılıç, Y.O. Use of waste glass powder toward more sustainable geopolymer concrete. *J. Mater. Res. Technol.* **2023**, *24*, 8533–8546. [CrossRef]
58. Mohammed, A.A.; Ahmed, H.U.; Mosavi, A. Survey of mechanical properties of geopolymer concrete: A comprehensive review and data analysis. *Materials* **2021**, *14*, 4690. [CrossRef] [PubMed]
59. Ren, Z.; Zeng, H.; Zeng, X.; Chen, X.; Wang, X. Effect of nanographite conductive concrete mixed with magnetite sand excited by different alkali activators and their combinations on the properties of conductive concrete. *Buildings* **2023**, *13*, 1630. [CrossRef]
60. Ma, C.K.; Awang, A.Z.; Omar, W. Structural and material performance of geopolymer concrete: A review. *Constr. Build Mater.* **2018**, *186*, 90–102. [CrossRef]
61. Pires, E.F.C.; De Azevedo, C.M.C.; Pimenta, A.R.; Da Silva, F.J.; Darwish, F.A.I. Fracture properties of geopolymer concrete based on metakaolin, fly ash and rice rusk ash. *Mater. Res.* **2017**, *20*, 630–636. [CrossRef]
62. Zhou, F.; Jiang, H.; Huang, L.; Hu, Y.; Xie, Z.; Zeng, Z.; Liu, M.; Wang, B.; Zhou, X. Early shrinkage modeling of complex internally confined concrete based on capillary tension theory. *Buildings* **2023**, *13*, 2201. [CrossRef]
63. Zhao, Q.; Nair, B.; Rahimian, T.; Balaguru, P. Novel geopolymer based composites with enhanced ductility. *J. Mater. Sci.* **2007**, *42*, 3131–3137. [CrossRef]
64. Ranjbar, N.; Mehrali, M.; Behnia, A.; Pordsari, A.J. A Comprehensive study of the polypropylene fiber reinforced fly ash based geopolymer. *PLoS ONE* **2016**, *11*, e0147546. [CrossRef] [PubMed]
65. Yusuf, T.O.; Ismail, M.; Usman, J.; Noruzman, A.H. Impact of blending on strength distribution of ambient cured metakaolin and palm oil fuel ash based geopolymer mortar. *Adv. Civ. Eng.* **2014**, *2014*, 658067. [CrossRef]
66. Singh, A.; Wang, Y.; Zhou, Y.; Sun, J.; Xu, X.; Li, Y.; Liu, Z.; Chen, J.; Wang, X. Utilization of antimony tailings in fiber-reinforced 3D printed concrete: A sustainable approach for construction materials. *Constr. Build. Mater.* **2023**, *408*, 133689. [CrossRef]
67. Çelik, A.L.I.; Özkılıç, Y.O. Geopolymer concrete with high strength, workability and setting time using recycled steel wires and basalt powder. *Steel Compos. Struct.* **2023**, *46*, 689–707.
68. Chen, L.; Chen, Z.; Xie, Z.; Wei, L.; Hua, J.; Huang, L.; Yap, P.-S. Recent developments on natural fiber concrete: A review of properties, sustainability, applications, barriers, and opportunities. *Dev. Built. Environ.* **2023**, *16*, 100255. [CrossRef]
69. Gerges, N.; Issa, C.A.; Sleiman, E.; Najjar, M.; Kattouf, A. Experimental study of the shear behavior of RC beams strengthened with high-performance fiber-reinforced concrete. *Int. J. Conc. Str. Mat.* **2023**, *17*, 17. [CrossRef]
70. Davidovits, J. Geopolymer cement to minimize carbon-dioxde greenhouse-warming. *Ceram. Trans.* **1993**, *37*, 165–182. Available online: https://www.researchgate.net/publication/284682578_Geopolymer_cement_to_minimize_carbon-dioxde_greenhouse-warming (accessed on 27 December 2022).
71. Nergis, D.D.B.; Abdullah, M.M.A.B.; Vizureanu, P.; Tahir, M.F.M. Geopolymers and their uses: Review. In *IOP Conference Series: Materials Science and Engineering*; IOP Publishing: Bristol, UK, 2018. [CrossRef]
72. Adam, A.A.; Horianto, X.X.X. The effect of temperature and duration of curing on the strength of fly ash based geopolymer mortar. *Procedia Eng.* **2014**, *95*, 410–414. [CrossRef]
73. Arulrajah, A.; Kua, T.-A.; Phetchuay, C.; Horpibulsuk, S.; Mahghoolpilehrood, F.; Disfani, M.M. Spent coffee grounds–fly ash geopolymer used as an embankment structural fill material. *J. Mater. Civ. Eng.* **2016**, *28*, 04015197. [CrossRef]
74. Deb, P.S.; Sarker, P.K. Effects of ultrafine fly ash on setting, strength, and porosity of geopolymers cured at room temperature. *J. Mater. Civ. Eng.* **2017**, *29*, 0001745. [CrossRef]
75. Alehyen, S.; El Achouri, M.; Taibi, M. Characterization, microstructure and properties of fly ash-based geopolymer. *J. Mater. Environ. Sci.* **2017**, *8*, 1783–1796.
76. Nikolov, A.; Rostovsky, I.; Nugteren, H. Geopolymer materials based on natural zeolite. *Case Stud. Constr. Mater.* **2017**, *6*, 198–205. [CrossRef]
77. Shilar, F.A.; Ganachari, S.V.; Patil, V.B.; Khan, T.M.Y.; Almakayeel, N.M.; Alghamdi, S. Review on the relationship between nano modifications of geopolymer concrete and their structural characteristics. *Polymers* **2022**, *14*, 1421. [CrossRef]
78. Özkılıç, Y.O.; Çelik, A.İ.; Tunç, U.; Karalar, M.; Deifalla, A.; Alomayri, T.; Althoey, F. The use of crushed recycled glass for alkali activated fly ash based geopolymer concrete and prediction of its capacity. *J. Mater. Res. Technol.* **2023**, *24*, 8267–8281. [CrossRef]
79. Davidovits, J. Geopolymers: Ceramic-like inorganic polymers. *J. Ceram. Sci. Technol.* **2017**, *8*, 335–350. [CrossRef]
80. Kamal, I.M.; Allaf, K. Geopolymers: Prospects for polymer industry geopolymers: Prospects for polymer industry. In Proceedings of the International Conference on Advances and Trends in Engineering Materials and Their Applications, Montréal, QC, Canada, 15–19 June 2015.
81. Khater, H.M. Studying the effect of thermal and acid exposure on alkaliactivated slag geopolymer. *Adv. Cem. Res.* **2014**, *26*, 1–9. [CrossRef]

82. Bakharev, T. Thermal behaviour of geopolymers prepared using class F fly ash and elevated temperature curing. *Cem. Concr. Res.* **2006**, *36*, 1134–1147. [CrossRef]
83. Sanusi, O.; Tempest, B.; Ogunro, V.O.; Gergely, J. Leaching characteristics of geopolymer cement concrete containing recycled concrete aggregates. *J. Hazard. Toxic Radioact. Waste* **2016**, *20*, 04016002. [CrossRef]
84. Hermann, E.; Kunze, C.; Gatzweiler, R.; Kießig, G.; Davidovits, J. Solidification of various radioactive residues by géopolymère® with special emphasis on long-term-stability. In Proceedings of the Geopolymers Conference, Saint-Quentin, France, 30 June–2 July 1999; pp. 211–228. Available online: http://www.wisutec.de/portals/9/publication/geopolymer_99.pdf (accessed on 27 December 2022).
85. Xu, H.; Van Deventer, J.S.J. The geopolymerisation of alumino-silicate minerals. *Int. J. Miner. Process.* **2000**, *59*, 247–266. [CrossRef]
86. Lippiatt, B.C.; Ahmad, S. Measuring the life-cycle environmental and economic performance of concrete: The bees approach. In Proceedings of the International Workshop on Sustainable Development and Concrete Technology, Beijing, China, 20–21 May 2004.
87. Duxson, P.; Fernández-Jiménez, A.; Provis, J.L.; Lukey, G.C.; Palomo, A.; Van Deventer, J.S.J. Geopolymer technology: The current state of the art. *J. Mater. Sci.* **2007**, *42*, 2917–2933. [CrossRef]
88. Fernández-Jiménez, A.; Palomo, A. Characterisation of fly ashes. Potential reactivity as alkaline cements. *Fuel* **2003**, *82*, 2259–2265. [CrossRef]
89. Chaklader, A.C.D.; Gupta, S.D.; Lin, E.C.Y.; Gutowski, B. Al_2O_3-SiC composites using alumino-silicate (natural and synthetic) precursor materials. *Solid State Phenom.* **1992**, *25–26*, 429–436. [CrossRef]
90. Fernández-Jiménez, A.; Palomo, A. Composition and microstructure of alkali activated fly ash binder: Effect of the activator. *Cem. Concr. Res.* **2005**, *35*, 1984–1992. [CrossRef]
91. Mikuni, A.; Komatsu, R.; Ikeda, K. Dissolution properties of some fly ash fillers applying to geopolymeric materials in alkali solution. *J. Mater. Sci.* **2007**, *42*, 2953–2957. [CrossRef]
92. Panagiotopoulou, C.; Kontori, E.; Perraki, T.; Kakali, G. Dissolution of aluminosilicate minerals and by-products in alkaline media. *J. Mater. Sci.* **2007**, *42*, 2967–2973. [CrossRef]
93. Ding, Y.; Dai, J.G.; Shi, C.J. Mechanical properties of alkali-activated concrete: A state-of-the-art review. *Constr. Build Mater.* **2016**, *127*, 68–79. [CrossRef]
94. Zhang, H.Y.; Kodur, V.; Wu, B.; Yan, J.; Yuan, Z.S. Effect of temperature on bond characteristics of geopolymer concrete. *Constr. Build. Mater.* **2018**, *163*, 277–285. [CrossRef]
95. Zulfiati, R.; Saloma; Idris, Y. The nature of coconut fibre fly ash-based mechanical geopolymer. In *IOP Conference Series: Materials Science and Engineering*; IOP Publishing: Bristol, UK, 2020. [CrossRef]
96. Samal, S.; Blanco, I. An application review of fiber-reinforced geopolymer composite. *Fibers* **2021**, *9*, 23. [CrossRef]
97. Lin, T.; Jia, D.; He, P.; Wang, M. In situ crack growth observation and fracture behavior of short carbon fiber reinforced geopolymer matrix composites. *Mater. Sci. Eng. A* **2010**, *527*, 2404–2407. [CrossRef]
98. Silva, L.C.; Ferreira, R.A.d.R.; Motta, L.A.d.C.; Machado, L.B. Optimization of metakaolin-based geopolymer composite using sisal fibers, response surface methodology, and canonical analysis. *Int. J. Adv. Eng. Res. Sci.* **2019**, *6*, 32–44. [CrossRef]
99. Catauro, M.; Tranquillo, E.; Barrino, F.; Poggetto, G.D.; Blanco, I.; Cicala, G.; Ognibene, G.; Recca, G. Mechanical and thermal properties of fly ash-filled geopolymers. *J. Therm. Anal. Calorim.* **2019**, *138*, 3267–3276. [CrossRef]
100. Samal, S. Effect of shape and size of filler particle on the aggregation and sedimentation behavior of the polymer composite. *Powder Technol.* **2020**, *366*, 43–51. [CrossRef]
101. Bai, T.; Liu, B.; Wu, Y.; Huang, W.; Wang, H.; Xia, Z. Mechanical properties of metakaolin-based geopolymer with glass fiber reinforcement and vibration preparation. *J. Non-Crystalline Solids* **2020**, *544*, 120173. [CrossRef]
102. Mallick, P.K. Thermoplastics and thermoplastic–matrix composites for lightweight automotive structures. In *Materials, Design and Manufacturing for Lightweight Vehicles*; Woodhead Publishing: Sawston, UK, 2021. [CrossRef]
103. Samal, S. Effect of high temperature on the microstructural evolution of fiber reinforced geopolymer composite. *Heliyon* **2019**, *5*, e01779. [CrossRef] [PubMed]
104. Samal, S.; Thanh, N.P.; Petríková, I.; Marvalová, B.; Vallons, K.A.M.; Lomov, S.V. Correlation of microstructure and mechanical properties of various fabric reinforced geo-polymer composites after exposure to elevated temperature. *Ceram. Int.* **2015**, *41*, 12115–12129. [CrossRef]
105. Samal, S.; Thanh, N.P.; Petríková, I.; Marvalová, B. Improved mechanical properties of various fabric-reinforced geocomposite at elevated temperature. *JOM* **2015**, *67*, 1478–1485. [CrossRef]
106. Ranjbar, N.; Zhang, M. Fiber-reinforced geopolymer composites: A review. *Cem. Concr. Compos* **2020**, *107*, 103498. [CrossRef]
107. Behbahani, H.; Nematollahi, B. Steel fiber reinforced concrete: A review. In Proceedings of the International Conference on Structural Engineering Construction and Management, Kandy, Sri Lanka, 19 December 2011; pp. 1–12.
108. Han, B.; Yu, X.; Ou, J. Compositions of self-sensing concrete. In *Self-Sensing Concrete in Smart Structures*; Butterworth-Heinemann: Oxford, UK, 2014. [CrossRef]
109. Panzera, T.H.; Christoforo, A.L.; Borges, P.H.R. High performance fibre-reinforced concrete (FRC) for civil engineering applications. In *Advanced Fibre-Reinforced Polymer (FRP) Composites for Structural Applications*; Woodhead Publishing: Sawston, UK, 2013. [CrossRef]
110. *A820*; Standard Specification for Steel Fibers for Fiber-Reinforced Concrete. ASTM: West Conshohocken, PA, USA, 2006.

111. Ganesan, N.; Abraham, R.; Raj, S.D. Durability characteristics of steel fibre reinforced geopolymer concrete. *Constr. Build Mater.* **2015**, *93*, 471–476. [CrossRef]
112. Mousavinejad, S.H.G.; Sammak, M. Strength and chloride ion penetration resistance of ultra-high-performance fiber reinforced geopolymer concrete. *Structures* **2021**, *32*, 1420–1427. [CrossRef]
113. Riahi, S.; Nemati, A.; Khodabandeh, A.R.; Baghshahi, S. Investigation of interfacial and mechanical properties of alumina-coated steel fiber reinforced geopolymer composites. *Constr. Build Mater.* **2021**, *288*, 123118. [CrossRef]
114. Shaikh, F.U.A. Review of mechanical properties of short fibre reinforced geopolymer composites. *Constr. Build Mater.* **2013**, *43*, 37–49. [CrossRef]
115. Farhan, N.A.; Sheikh, M.N.; Hadi, M.N.S. Experimental investigation on the effect of corrosion on the bond between reinforcing steel bars and fibre reinforced geopolymer concrete. *Structures* **2018**, *14*, 251–261. [CrossRef]
116. Liu, Y.; Zhang, Z.; Shi, C.; Zhu, D.; Li, N.; Deng, Y. Development of ultra-high performance geopolymer concrete (UHPGC): Influence of steel fiber on mechanical properties. *Cem. Concr. Compos.* **2020**, *112*, 103670. [CrossRef]
117. Wang, Y.; Aslani, F.; Valizadeh, A. An investigation into the mechanical behaviour of fibre-reinforced geopolymer concrete incorporating NiTi shape memory alloy, steel and polypropylene fibres. *Constr. Build Mater.* **2020**, *259*, 119765. [CrossRef]
118. Liu, Y.; Shi, C.; Zhang, Z.; Li, N.; Shi, D. Mechanical and fracture properties of ultra-high performance geopolymer concrete: Effects of steel fiber and silica fume. *Cem. Concr. Compos.* **2020**, *112*, 103665. [CrossRef]
119. Ibraheem, M.; Butt, F.; Waqas, R.M.; Hussain, K.; Tufail, R.F.; Ahmad, N.; Usanova, K.; Musarat, M.A. Mechanical and microstructural characterization of quarry rock dust incorporated steel fiber reinforced geopolymer concrete and residual properties after exposure to elevated temperatures. *Materials* **2021**, *14*, 6890. [CrossRef] [PubMed]
120. Tran, T.T.; Pham, T.M.; Hao, H. Experimental and analytical investigation on flexural behaviour of ambient cured geopolymer concrete beams reinforced with steel fibers. *Eng. Struct.* **2019**, *200*, 109707. [CrossRef]
121. Their, J.M.; Özakça, M. Developing geopolymer concrete by using cold-bonded fly ash aggregate, nano-silica, and steel fiber. *Constr. Build Mater.* **2018**, *180*, 12–22. [CrossRef]
122. Khan, M.Z.N.; Hao, Y.; Hao, H.; Shaikh, F.U.A. Mechanical properties of ambient cured high strength hybrid steel and synthetic fibers reinforced geopolymer composites. *Cem. Concr. Compos.* **2018**, *85*, 133–152. [CrossRef]
123. Shaikh, F.U.A.; Hosan, A. Mechanical properties of steel fibre reinforced geopolymer concretes at elevated temperatures. *Constr. Build Mater.* **2016**, *114*, 15–28. [CrossRef]
124. Ng, T.S.; Amin, A.; Foster, S.J. The behaviour of steel-fibrereinforced geopolymer concrete beams in shear. *Mag. Concr. Res.* **2013**, *65*, 308–318. [CrossRef]
125. Ganesh, A.C.; Sowmiya, K.; Muthukannan, M. Investigation on the effect of steel fibers in geopolymer concrete. In *IOP Conference Series: Materials Science and Engineering*; IOP Publishing: Bristol, UK, 2020. [CrossRef]
126. Elkholy, S.; El-Hassan, H. Mechanical and micro-structure characterization of steel fiber-reinforced geopolymer concrete. In Proceedings of the ISEC 2019—10th International Structural Engineering and Construction Conference, Chicago, IL, USA, 20–25 May 2019; pp. 1–6. [CrossRef]
127. Islam, A.; Alengaram, U.J.; Jumaat, M.Z.; Ghazali, N.B.; Yusoff, S.; Bashar, I.I. Influence of steel fibers on the mechanical properties and impact resistance of lightweight geopolymer concrete. *Constr. Build Mater.* **2017**, *152*, 964–977. [CrossRef]
128. Ganesan, N.; Indira, P.V.; Santhakumar, A. Influence of steel fibres on tension stiffening and cracking of reinforced geopolymer concrete. *Mag. Concr. Res.* **2014**, *66*, 268–276. [CrossRef]
129. Pham, K.V.A.; Nguyen, T.K.; Le, T.A.; Han, S.W.; Lee, G.; Lee, K. Assessment of performance of fiber reinforced geopolymer composites by experiment and simulation analysis. *Appl. Sci.* **2019**, *9*, 3424. [CrossRef]
130. Saranya, P.; Nagarajan, P.; Shashikala, A.P. Performance studies on steel fiber—Reinforced GGBS-dolomite geopolymer concrete. *J. Mater. Civ. Eng.* **2021**, *33*, 04020447. [CrossRef]
131. Park, S.J.; Seo, M.K. Element and processing. *Interface Sci. Technol.* **2011**, *18*, 431–499. [CrossRef]
132. Zweben, C.H. *Composites: Overview, Encyclopedia of Condensed Matter Physics*; Elsevier: Amsterdam, The Netherlands, 2005; pp. 192–208. [CrossRef]
133. Kumar, Y.N.; Kumar, B.D.; Swami, B.L.P. Mechanical properties of geopolymer concrete reinforced with steel and glass fibers with various mineral admixtures. *Mater. Today Proc.* **2022**, *52*, 632–641. [CrossRef]
134. Sivaraja, M.; Murugesan, J.; Manickam, H.; Ramasamy, K. Performance of glass fiber reinforced geopolymer concrete under varying temperature effect. *Technology* **2018**, *9*, 1316–1323.
135. Alomayri, T.; Adesina, A. The influence of nano $CaCO_3$ on the mechanical performance of micro glass-reinforced geopolymer paste. *Arab. J. Geosci.* **2021**, *14*, 1–7. [CrossRef]
136. Sathanandam, T.; Awoyera, P.O.; Vijayan, V.; Sathishkumar, K. Low carbon building: Experimental insight on the use of fly ash and glass fibre for making geopolymer concrete. *Sustain. Environ. Res.* **2017**, *27*, 146–153. [CrossRef]
137. Nematollahi, B.; Sanjayan, J.; Xia, J.; Chai, H.; Lu, T.M. Properties of fresh and hardened glass fiber reinforced fly ash based geopolymer concrete. *Key Eng. Mater.* **2014**, *595*, 629–633. [CrossRef]
138. Ganesh, A.C.; Muthukannan, M. Development of high performance sustainable optimized fiber reinforced geopolymer concrete and prediction of compressive strength. *J. Clean Prod.* **2021**, *282*, 124543. [CrossRef]
139. Zuaiter, M.; El-Hassan, H.; El-Maaddawy, T.; El-Ariss, B. Properties of slag-fly ash blended geopolymer concrete reinforced with hybrid glass fibers. *Buildings* **2022**, *12*, 1114. [CrossRef]

140. Kumar, R.; Suman, S.K.; Sharma, M. Laboratory investigation on the synthesis and mechanical characterization of fiber reinforced geopolymer concrete. *Mater. Today Proc.* **2019**, *32*, 268–273. [CrossRef]
141. Ali, S.; Sheikh, M.N.; Hadi, M.N.S. Behavior of axially loaded plain and fiber-reinforced geopolymer concrete columns with glass fiber-reinforced polymer cages. *Struct. Concr.* **2021**, *22*, 1800–1816. [CrossRef]
142. Abbas, S.N.; Qureshi, M.I.; Abid, M.M.; Zia, A.; Tariq, M.A.U.R. An Investigation of mechanical properties of fly ash based geopolymer and glass fibers concrete. *Sustainability* **2022**, *14*, 10489. [CrossRef]
143. Saral, J.A.; Gayathri, S.; Tamilselvi, M.; Raj, B.R. An experimental study on fibre reinforced geopolymer concrete composites-glass fibre, copper slag. *Int. J. Eng. Technol.* **2018**, *7*, 433–435. [CrossRef]
144. Mehta, S.; Bhandari, M. Effect of glass fiber and recycled aggregates on Geopolymer concrete. In *IOP Conference Series: Earth and Environmental Science*; IOP Publishing: Bristol, UK, 2021. [CrossRef]
145. Reed, M.; Lokuge, W.; Karunasena, W. Fibre-reinforced geopolymer concrete with ambient curing for in situ applications. *J. Mater. Sci.* **2014**, *49*, 4297–4304. [CrossRef]
146. Ranjbar, N.; Talebian, S.; Mehrali, M.; Kuenzel, C.; Metselaar, H.S.C.; Jumaat, M.Z. Mechanisms of interfacial bond in steel and polypropylene fiber reinforced geopolymer composites. *Compos. Sci. Technol.* **2016**, *122*, 73–81. [CrossRef]
147. Rajak, M.; Rai, B. Effect of micro polypropylene fibre on the performance of fly ash-based geopolymer concrete. *J. Appl. Eng. Sci.* **2019**, *9*, 97–108. [CrossRef]
148. Aygörmez, Y.; Canpolat, O.; Al-mashhadani, M.M.; Uysal, M. Elevated temperature, freezing-thawing and wetting-drying effects on polypropylene fiber reinforced metakaolin based geopolymer composites. *Constr. Build Mater.* **2020**, *235*, 117502. [CrossRef]
149. Maras, M.M.; Kose, M.M. Mechanical and microstructural properties of polypropylene fiber-reinforced geopolymer composites. *J. Fiber Sci. Technol.* **2019**, *75*, 35–46. [CrossRef]
150. Arunkumar, K.; Muthukannan, M.; Babu, A.D.; Hariharan, A.L.; Muthuramalingam, T. Effect on addition of polypropylene fibers in wood ash-fly ash based geopolymer concrete. In *IOP Conference Series: Materials Science and Engineering*; IOP Publishing: Bristol, UK, 2020. [CrossRef]
151. Chindaprasirt, P.; Boonbamrung, T.; Poolsong, A.; Kroehong, W. Effect of elevated temperature on polypropylene fiber reinforced alkali-activated high calcium fly ash paste. *Case Stud. Constr. Mater.* **2021**, *15*, e00554. [CrossRef]
152. Utami, F.A.R.; Triwiyono, A.; Agustini, N.K.A.; Perdana, I. Thermal conductivity of geopolymer with polypropylene fiber. In *IOP Conference Series: Materials Science and Engineering*; IOP Publishing: Bristol, UK, 2020. [CrossRef]
153. Mahltig, B. Basalt fibers. In *Inorganic and Composite Fibers: Production, Properties, and Applications*; Elsevier: Amsterdam, The Netherlands, 2018; pp. 195–217. [CrossRef]
154. Jamshaid, H.; Mishra, R. A green material from rock: Basalt fiber—A review. *J. Text. Inst.* **2016**, *107*, 923–937. [CrossRef]
155. Colombo, C.; Vergani, L.; Burman, M. Static and fatigue characterisation of new basalt fibre reinforced composites. *Compos. Struct.* **2012**, *94*, 1165–1174. [CrossRef]
156. King, M.F.L.; Srinivasan, V.; Purushothaman, T. Basalt fiber: An ancient material for innovative and modern application. *Middle-East J. Sci. Res.* **2014**, *22*, 308–312.
157. Ronad, A.; Karikatti, V.B.; Dyavanal, S.S. A study on mechanical properties of geopolymer concrete reinforced with basalt fiber. *Int. J. Res. Eng. Technol.* **2016**, *5*, 474–478. [CrossRef]
158. Wang, Y.; Hu, S.; He, Z. Mechanical and fracture properties of geopolymer concrete with basalt fiber using digital image correlation. *Theor. Appl. Fract. Mech.* **2021**, *112*, 102909. [CrossRef]
159. Temuujin, J.; Darkhijav, B. Influence of basalt fibres on the properties of fly ash based geopolymer concrete. *J. Part Aerosol. Res.* **2016**, *12*, 43–50.
160. Meguid, S.A.; Kosior-kazberuk, M.; Krassowska, J. Post-cracking behaviour of basalt fibre reinforced. In Proceedings of the 6th International Conference on Mechanics and Materials in Design: M2D2015, Ponta Delgada, Portugal, 26–30 July 2015; pp. 26–30.
161. Abbass, M.; Singh, G. Fatigue analysis of rice husk ash and basalt fibre-based sustainable geopolymer concrete in rigid pavements. *Mater. Today Proc.* **2021**, *45*, 5014–5022. [CrossRef]
162. Şahin, F.; Uysal, M.; Canpolat, O.; Aygörmez, Y.; Cosgun, T.; Dehghanpour, H. Effect of basalt fiber on metakaolin-based geopolymer mortars containing rilem, basalt and recycled waste concrete aggregates. *Constr. Build Mater.* **2021**, *301*, 124113. [CrossRef]
163. Shaikh, F.; Haque, S. Behaviour of carbon and basalt fibres reinforced fly ash geopolymer at elevated temperatures. *Int. J. Concr. Struct. Mater.* **2018**, *12*, 35. [CrossRef]